European Journal of Taxonomy 987: 98–145
https://doi.org/10.5852/ejt.2025.987.2867
ISSN 2118-9773
www.europeanjournaloftaxonomy.eu
2025 · Griebenow Z.H. *et al.*

Research article

urn:lsid:zoobank.org:pub:4EFDA262-1072-4734-91FB-66B60E4263B5

Four new species of Leptanillinae (Hymenoptera: Formicidae) from northern Vietnam described with phylogenomics and micro-computed tomography

Zachary Hayes GRIEBENOW [1,*], Adrian RICHTER [2], Evan P. ECONOMO [3], An Van DANG [4] & Aiki YAMADA [5]

[1] USDA ARS Systematic Entomology Laboratory, c/o National Museum of Natural History, Constitution Avenue, 10th St. and Constitution Ave. NW, Washington D.C. 20013, USA.
[1] University of California, One Shields Avenue, Davis 95616, California, USA.
[1] C.P. Gillette Museum, Colorado State University, 600 Hughes Way, Fort Collins 80523, Colorado, USA.
[2] Senckenberg Research Institute & Natural History Museum, Senckenberganlage 25, Frankfurt am Main 60325, Germany.
[2,3] Biodiversity & Biocomplexity Unit, Okinawa Institute of Science & Technology Graduate University, Onna-son, Okinawa, 904-0495, Japan.
[4,5] Systematic Zoology Laboratory, Department of Biological Sciences, Graduate School of Science, Tokyo Metropolitan University, 1-1 Minami-Osawa, Hachioji, Tokyo, 192-0397, Japan.
[4] Institute of Ecology and Biological Resources, Vietnam Academy of Science and Technology, 18, Hoang Quoc Viet, Cau Giay, Hanoi, Vietnam.
[5] Department of Medical Entomology, National Institute of Infectious Diseases, Toyama 1-23-1, Shinjuku, Tokyo 162-8640, Japan.

[*] Corresponding author: zachary.griebenow@colostate.edu
[2] Email: adrian.richter@senckenberg.de
[3] Email: evaneconomo@gmail.com
[4] Email: dvaniebr@gmail.com
[5] Email: aiki.ymd@gmail.com

[1] urn:lsid:zoobank.org:author:8221CF5F-DC93-4B34-A527-F48721D23F5E
[2] urn:lsid:zoobank.org:author:F74539D8-1606-4D8D-98EB-F84C67C773E0
[3] urn:lsid:zoobank.org:author:F547928C-E9EE-4B6C-8F80-8C11467A19F6
[4] urn:lsid:zoobank.org:author:B9D6E28E-9504-40D0-830E-5C525E944E26
[5] urn:lsid:zoobank.org:author:D5CE59FA-1886-4C95-927C-6256E97328AE

Abstract. The enigmatic ants of the subfamily Leptanillinae (Hymenoptera: Formicidae) are rarely collected, being minute and largely subterranean in biology. Vietnam is one of only two countries from which all three leptanilline genera are recorded; yet, only one described species has so far been reported from the country (*Opamyrma hungvuong* Yamane *et al.*, 2008). Here, we describe four new species of Leptanillinae from Vietnam: *Protanilla rong* sp. nov., *Leptanilla belantanoides* sp. nov., *Leptanilla sapa* Yamada sp. nov., and *Leptanilla phthirigyna* sp. nov. We present the first detailed description of the larva of *Protanilla* (*Protanilla rong*); and of the male and gyne of *Protanilla gengma* Xu, 2012,

the first time these forms have been described for the *Protanilla bicolor* species-group. We include volumetric reconstructions of the worker caste in *Leptanilla charonea* Barandica *et al.*, 1994, *Leptanilla belantanoides*, *Leptanilla sapa*, *Protanilla rong*, and the gyne of the latter two species, derived from micro-computed tomography (μ-CT); and present the results of maximum-likelihood and Bayesian phylogenomic inference with the most comprehensive sampling of the Leptanillinae yet published. We also associate the male and worker of *Leptanilla belantanoides* by phylogenomics, providing the first such linkage for any species of the *Leptanilla thai* species-group; and resolve the phylogenetic placement of the bizarre *Protanilla izanagi* Terayama, 2013. Volumetric reconstruction of frontoclypeal skeletomusculature in *Leptanilla* via μ-CT elucidates anterior cranial anatomy in that genus.

Keywords. Micro-CT, *Protanilla bicolor* species-group, *Protanilla izanagi*, *Protanilla gengma*, clypeal process.

Griebenow Z.H., Richter A., Economo E.P., Dang A.v. & Yamada A. 2025. Four new species of Leptanillinae (Hymenoptera: Formicidae) from northern Vietnam described with phylogenomics and micro-computed tomography. *European Journal of Taxonomy* 987: 98–145. https://doi.org/10.5852/ejt.2025.987.2867

Introduction

The enigmatic ant subfamily Leptanillinae Emery, 1910 is a clade of minute, subterranean centipede predators (Masuko 1990; Hsu *et al.* 2017; Yamada *et al.* 2023) consisting of three genera (*Opamyrma* Yamane *et al.*, 2008, *Protanilla* Taylor, 1990, and *Leptanilla* Emery, 1870) known from tropical to warm temperate regions of the Old World. The Leptanillinae are sister to the Martialinae, with which they form a clade sister to all other extant ants (Rabeling *et al.* 2008; Kück *et al.* 2011; Borowiec *et al.* 2019; Romiguier *et al.* 2022). Recent integrative systematic revision of the Leptanillinae has ensured reciprocal monophyly of higher taxa (Griebenow 2021, 2024; Griebenow *et al.* 2022), but the species-level taxonomy of the group is far from complete, with Southeast Asia hosting a wealth of undescribed morphospecies known only from male specimens.

Vietnam lies on the eastern part of the Indochinese Peninsula and is known for its rich biodiversity (Sterling *et al.* 2008). The myrmecofauna of Vietnam is accordingly diverse, with 434 species recorded (Guénard *et al.* 2017), and harbors areas in the top 10% globally for ant species richness and rarity (Kass *et al.* 2022). Vietnam is therefore a predicted hotspot for discovery of new ant species. Accordingly, Vietnam appears to be a global center of diversity for the Leptanillinae, along with China one of only two states from which all three leptanilline genera have been recorded. Several species were previously reported from Vietnam (Eguchi *et al.* 2014), but of them only *Opamyrma hungvuong* Yamane *et al.*, 2008 has been formally described so far.

Here, we describe four new species of the tribe Leptanillini Emery, 1910 from northern Vietnam, representing the *Protanilla rafflesi* species-group (*Protanilla rong* sp. nov.; worker, gyne, larva), the *Leptanilla thai* species-group (*Leptanilla belantanoides* sp. nov. [worker, male] and *Leptanilla sapa* Yamada sp. nov. [worker, gyne]), and the *Leptanilla revelierii* species-group (*Leptanilla phthirigyna* sp. nov.; worker, gyne). In addition, we describe the gyne and male of *Protanilla gengma* Xu, 2012, with this being the first description of these forms for the *Protanilla bicolor* species-group, illuminating the male genital morphology of one of the only major clades of Leptanillini not examined by Griebenow *et al.* (2023); and describe the larva of *Protanilla rong* in detail, this being the first such description for *Protanilla*. Four of these species are documented from the limestone evergreen tropical forest of Cuc Phuong National Park, a frequented location for biodiversity studies in Vietnam (Duwe *et al.* 2022), with previous comprehensive surveys noting 160 ant species, yet not detecting any Leptanillinae (Yamane *et al.* 2002; Eguchi *et al.* 2014).

Our descriptions are informed by maximum-likelihood (ML) and Bayesian phylogenomic inference from ultra-conserved elements (UCEs) with taxon sampling more comprehensive than any previous phylogenetic study of the Leptanillinae, indirectly associating the disparate worker and male of *L. belantanoides* sp. nov. Our phylogenetic inferences resolve the placement of the enigmatic Japanese endemic *Protanilla izanagi* Terayama, 2013 and imply that close relatives of this bizarre species exist throughout eastern Asia, including Vietnam. Our findings establish Vietnam as a center of previously undocumented high alpha- and beta-diversity within the Leptanillinae and expand scientific knowledge of these cryptic ants. Finally, μ-CT of the cranium in *L. belantanoides* sp. nov. and an Iberian representative of the *Leptanilla revelierii* species-group (*Leptanilla charonea* Barandica *et al.*, 1994) illuminates the heretofore-unclear anatomical origin of the anterior cranial process in *Leptanilla*.

Material and methods

Terminology and species concept

Morphological terminology follows the sources cited by Griebenow (2024: 89–90) and is summarized by Griebenow (2024: figs 1–2, 29, 31, 38). Skeletomuscular terminology follows Beutel *et al.* (2014) and Richter *et al.* (2020). We consider species to be evolutionarily independent metapopulations, distinct in genotype and phenotype from other such lineages (Barraclough 2019).

Specimen repositories

Specimens consulted in this study are deposited at the following institutions, marked with an asterisk if not listed on the Global Registry of Scientific Collections:

CASC = California Academy of Sciences, San Francisco, USA
CSCA = California State Collection of Arthropods, Sacramento, USA
HKU = University of Hong Kong, China
HUI = University of Isfahan, Isfahan, Iran
IEBR = Institute of Ecology & Biological Resources, Vietnam Academy of Science & Technology, Ha Noi, Vietnam
MCZ = Museum of Comparative Zoology, Cambridge, USA
LUND = Lund University Biological Museum, Lund, Sweden
*NCUE = National Changhua University of Education, Changhua, Taiwan
OIST = Okinawa Institute of Science and Technology, Onna-son, Japan
ROM = Royal Ontario Museum, Toronto, Canada
UCDC = R.M. Bohart Museum of Entomology, University of California, Davis, USA

We also examined material from the personal collections of Katsuyuki Eguchi, Philip Ward, and José María Gómez-Durán. Relevant data for specimens newly sequenced in this study are provided in Supp. file 1. All collection data for these specimens are provided on AntWeb.

Measurements

EL = Eye Length, maximum length of compound eye in profile view measured parallel to anteroposterior axis of head
EW = Eye Width, maximum breadth of compound eye in profile view measured perpendicular to anteroposterior axis of head
HL = Head Length, maximum length of head in full-face view from anterior margin of head capsule to cranial vertex, including ocelli if present
HW = Head Width, maximum width of cranium in full-face view, including compound eyes if present
LF2 = Third Antennomere Length, length of the basal flagellomere

MaL = Mandalar Length, maximum length of mandalus, measured along proximodistal axis of mandible
ML = Mandible Length, maximum length of mandible from view orthogonal to lateral mandibular margin, measured from ventral mandibular articulation to mandibular apex
MW = Mesosomal width, maximum width of mesosoma inclusive of mesopectus (if visible) in dorsal view, measured immediately anterior to mesocoxal foramina
PPH = Postpetiolar height, maximum height of postpetiole in profile view and perpendicular to PPL, including sternal process and dorsal node, if distinct
PPL = Postpetiolar length, maximum length of postpetiole in dorsal view, excluding presclerites and including posterior collar
PPW = Postpetiolar width, maximum width of postpetiole in dorsal view
PrW = Pronotal width, maximum width of pronotum, measured in dorsal view
PTH = Petiolar height, maximum height of petiole in profile view and perpendicular to PTL, including sternal process and dorsal node, if distinct
PTL = Petiolar length, maximum length of petiole in dorsal view, excluding presclerites and including posterior collar
PTW = Petiolar width, maximum width of petiole in dorsal view and orthogonal to anteroposterior axis
SL = Scape Length, maximum length of scape in medial view, excluding bulbus and including distal articulatory laminae
TW4 = Width of abdominal tergite IV, maximum width of abdominal tergite IV measured in dorsal view
WL = Weber's Length, maximum diagonal distance measured from most anterior extent of pronotum excluding (worker) or including (gyne, male) cervical shield to most posteroventral extremity of the mesosoma, including propodeal lobes if present

Indices

CI = (HW/HL) × 100
MI = (ML/HW) × 100
MSI = (MSW/MSL) × 100
OI = (EW/EL) × 100
PI = (PTW/PTL) × 100
PPI = (PPW/PPL) × 100
REL = (EL/HL) × 100
SI = (SL/HW) × 100
TI1 = (PPW/TW4) × 100

Sequencing and phylogenetic inference

Taxon sampling in this study expands on previous phylogenomic representation (Griebenow 2020; Griebenow *et al.* 2022) across the whole of the Leptanillinae, with a total of 85 sequences, but particularly focuses on the *Leptanilla revelierii* species-group and *Leptanilla thai* species-group, which are by far the most speciose major clades among the Leptanillinae. For the 34 sequences newly published in this study (Supp. file 1), DNA was extracted non-destructively using a DNeasy Blood & Tissue Kit (Qiagen Inc., Valencia, CA) either according to manufacturer instructions, or with DNA eluted using buffer AE at 56°C (Cruaud *et al*. 2019). Genomic concentrations were quantified for each sample with a Qubit 2.0 fluorometer (Life Technologies Inc., Carlsbad, CA). Input DNA was sheared to ~600 bp using a QSonica Q800R3-110 (Qsonica Inc., Newtown, CT). Sheared product was used as input for the modified library preparation protocol of Branstetter *et al*. (2017) involving SPRI bead cleanup with a generic substitute (Rohland & Reich 2012) and custom dual-indexing barcodes (Glenn *et al.* 2019) with phylogenomic

data generated using the ant-specific version of the UCE probe set *hym-v2* (Branstetter *et al.* 2017). Enrichment success and size-adjusted DNA concentrations of pools were assessed using the SYBR FAST qPCR kit (Kapa Biosystems, Wilmington, MA), and all pools were combined into an equimolar final pool. For 11 samples, libraries were prepared and enriched using similar protocols at RAPiD Genomics LLC (Gainesville, FL). Final pools were sequenced on an Illumina HiSeq X at Novogene (Sacramento, CA), at Rapid Genomics, or on an Illumina HiSeq 2500 at the University of Utah Huntsman Cancer Institute (Salt Lake City, UT). Sequence Read Archive (SRA) accession codes for all raw reads used in this study are included in Supp. file 1. Sequence data for the 56 UCE datasets published previously to this study are derived from Griebenow (2020) and Griebenow *et al*. (2022), and sequencing protocols for these data can be found therein.

The FASTQ output was demultiplexed and cleansed of adapter contamination and low-quality reads using *illumiprocessor* (Faircloth 2016) in the PHYLUCE package, ver. 1.6.7, on Ubuntu ver. 22.04.1 LTS. Raw reads were assembled with SPAdes ver. 3.12.0 (Bankevich *et al.* 2012). Subsequent PHYLUCE commands were implemented on Ubuntu Linux ver. 20.04. Species-specific contig assemblies were obtained with the ant-specific *hym-v2* probe set (Branstetter *et al.* 2017) using *phyluce_assembly_match_contigs_to_probes.py* (min_identity=80); and a list of UCE loci shared across all taxa was generated using *phyluce_assembly_get_match_counts.py*, and separate FASTA files for each locus were created using these outputs. In this study, all loci are necessarily UCEs, and therefore the terms are synonymous herein. Sequences were aligned separately by locus using MAFFT (Katoh & Toh 2010) implemented with the command *phyluce_assembly_seqcap_align.py*. These sequences were then trimmed with Gblocks (Castresana 2000) as implemented by the wrapper script *phyluce_assembly_get_gblocks_trimmed_alignment_from_untrimmed.py* (settings: b1 = 0.5, b2 = 0.5, b3 = 12, b4 = 7). Locus names were removed from taxon labels with *phyluce_align_remove_locus_name_from_files.py* and the final alignment created by *phyluce_align_get_only_loci_with_min_taxa.py* with the minimum percentage of taxa represented in each locus being 90%, resulting in an alignment of 534 loci (343 184 bp total). Summary statistics for this alignment were calculated using AMAS (Borowiec 2016).

Spruceup (Borowiec 2019) was used to trim potentially misaligned sequences in the final matrix. Genetic distances are calculated by Spruceup among sequences within alignment intervals of predefined length and overlap, with a log-normal curve being fitted to these distances; outliers along this distribution are then eliminated according to a predefined threshold. To assess the effect of variation in cutoff, all maximum-likelihood (ML) phylogenetic inference was replicated with alignments trimmed in Spruceup according to four arbitrary lognormal cutoff values – 0.95, 0.90, 0.85, and 0.80, listed here from least to most strict – plus with said alignment untrimmed (i.e., lognormal cutoff value = 1).

Maximum-likelihood phylogenomic inference was implemented in IQ-Tree ver. 2.1.2 (Minh *et al.* 2020) on the CIPRES Science Gateway (Miller *et al.* 2010), partitioned by locus (Chernomor *et al.* 2016) with substitution models and optimal partitioning scheme selected with the Bayesian information criterion (BIC) in ModelFinder (Kalyaanamoorthy *et al.* 2017). The conclusions of past phylogenomic inference focused the Leptanillinae have been robust to partitioning within UCEs (Griebenow 2020; Griebenow *et al.* 2022), so we did not implement any alternative partitioning schemes in this study. Substitution models considered in these analyses included those that model among-site rate variation by both the proportion of invariable sites (+I) and gamma-distributed (+G) extensions in conjunction (i.e., I+G), because IQ-Tree compensates for the statistical non-identifiability of substitution models with the I+G extension (Yang 1996; Nguyen *et al.* 2018). All ML analyses in IQ-Tree ran for 5000 ultrafast bootstrap (UFBoot) replicates (Hoang *et al.* 2018).

The favored partitioning scheme recovered by IQ-Tree for the alignment trimmed under a 0.90 lognormal threshold in Spruceup was used for partitioned Bayesian phylogenomic inference in ExaBayes ver. 1.5.1

(Aberer *et al.* 2014) on the CIPRES Science Gateway. Four independent runs were implemented for each analysis for 1 000 000 generations, with a pair of Markov-chain Monte Carlo (MCMCs) being implemented for each run. Default prior probability distributions were used for continuous parameters, with branch lengths being treated as unlinked across partitions. Initial topology was inferred with maximum parsimony (MP). The initial 25% of output was discarded as burn-in. MCMCs were considered to have converged with respect to topology, and analysis terminated, when either the average or mean standard deviation of split frequencies < 0.05. Continuous parameters were considered to have converged if ESS > 200 in Tracer ver. 1.7.2 (Rambaut *et al.* 2018). All input for ML and Bayesian phylogenomic inference, and resulting output, is provided on Zenodo (https://zenodo.org/records/10950468).

Imaging and µ-CT

Non-coating scanning electron microscopy (SEM) was performed with a Hitachi TM4000 (Hitachi Global, Tokyo, Japan). Coating SEM was performed with a JEOL JSM-7900F (JEOL Ltd., Tokyo, Japan) after freeze-drying from tert-Butyl ethanol with a Hitachi ES-2030 freeze-dryer. Photomicrography and image-stacking were undertaken using the same equipment and software as in Griebenow (2020, 2021, 2024), with the addition of four new imaging systems: a Canon EoS 5D camera (Canon Inc., Tokyo, Japan) operated with Capture One Pro ver. 9.2 (Capture One, Frederiksburg, Denmark) with *z*-stacking via Visionary Digital Passport (Visionary Digital Enterprises LLC, West Hollywood, CA), with focus stacking in Zerene Stacker ver. 1.04 (Zerene Systems LLC, Richland, WA); a Leica DMC5400 (Leica Camera AG, Wetzlar, Germany) camera mounted on a Leica M205 C microscope, operated with the Leica Application Suite X ver. 3.7.3.23245, including automated *z*-stacking; a Canon EOS R10 mirrorless camera mounted on a Nikon AZ100 microscope (Nikon Corporation, Tokyo, Japan), with manual focus-stacking in Affinity Photo 2 (Serif [Europe] Ltd., West Bridgford, United Kingdom); and a Nikon Z5 mirrorless camera mounted on a Nikon Eclipse E600, with manual focus stacking in Focus Pro ver. 8.2.2 (Helicon Soft, Kharkiv, Ukraine).

Micro-CT scanning was performed using a ZEISS Xradia 510 Versa 3D X-ray microscope (Carl Zeiss AG, Oberkochen, Germany) operated with the ZEISS Scout-and-Scan Control System software (ver. 11.1.6411.17883). Specimens were immersed in a 2 M iodine solution for 1–3 weeks, then washed for ≥ 1 hours in 99% ethanol mounted in a pipette tip for scanning. Whole-body scans were performed for all specimens at 50–80 kV and 4–7 W, with 5–15 seconds of exposure depending on specimen size. Voxel sizes of the scans range between 0.64 µm^3 and 1.4 µm^3 (Supp. file 2). 3D volumes were reconstructed from tomographic images using the Zeiss Scout-and-Scan Control System Reconstructor (ver. 11.1.6411.17883) and exported as .txm files. Scan data are provided on Zenodo (https://zenodo.org/records/10950468).

Three-dimensional volumes were imported into Amira 2020 (Visage Imaging GmbH, Berlin, Germany). We generated isosurfaces and exported them as .ply files. To generate surfaces of the head capsule, we employed semiautomatic segmentation using *biomedisa* (Lösel *et al.* 2020) before isosurface generation. For further processing, we used Meshlab (Cignoni *et al.* 2008), where we generated ambient occlusion, deleted internal faces and isolated pieces, and subsequently further reduced the surface through several cycles of "HC Laplacian Smooth and Simplification: Quadratic Edge Collapse Decimations" function. These volumetric reconstructions are available on SketchFab (https://skfb.ly/oTACt).

Results

Phylogenomic inference

All continuous parameters in our Bayesian analysis appeared to have converged (ESS > 200). The results of ML and Bayesian phylogenomic inference here corroborate previous phylogenomic studies of the

Leptanillinae (Griebenow 2020; Griebenow *et al.* 2022) and each other, with ML results being robust to varied trimming intensity in Spruceup. Bayesian posterior probabilities (BPP) are maximal, or nearly so, for all inferred nodes (Figs 1–2). Ultrafast bootstrap (UFBoot) values were likewise high for nearly all nodes, excepting a few tipward internal ones and the interrelationships of the major lineages of *Protanilla* (UFBoot = 58–95). Unless otherwise stated, all results referred to below received maximal statistical support (i.e., UFBoot = 100; BPP = 1) (https://zenodo.org/records/10950468).

Protanilla is divided into four lineages, three of which correspond to the species-groups delimited by Griebenow (2024). The fourth consists of *Protanilla izanagi*, known only from the female castes, and the undescribed male singleton *Protanilla* zhg-th02 (Fig. 1). Phenotype in these two representatives falls outside the worker- and male-based diagnoses for the remaining species-groups of *Protanilla* (Griebenow 2024), and so these two terminals are here together informally designated the *Protanilla izanagi* species-group. ML inference places this clade as sister to the *Protanilla bicolor* species-group with relatively high support (UFBoot = 92–95), a conclusion corroborated by Bayesian inference.

Maximum-likelihood and Bayesian inference agree with previous phylogenomic inference focused on the Leptanillinae, and these results (Figs 1–2) form the phylogenetic foundation for the taxonomic actions of Griebenow (2024).

Protanilla boltoni (Borowiec *et al.*, 2011), the sole sampled representative of the *Protanilla taylori* species-group (i.e., the former *Anomalomyrma*), is recovered as sister to the *Protanilla rafflesi* species-group; but ML analyses only give this hypothesis weak support (UFBoot = 58–81). ML and Bayesian

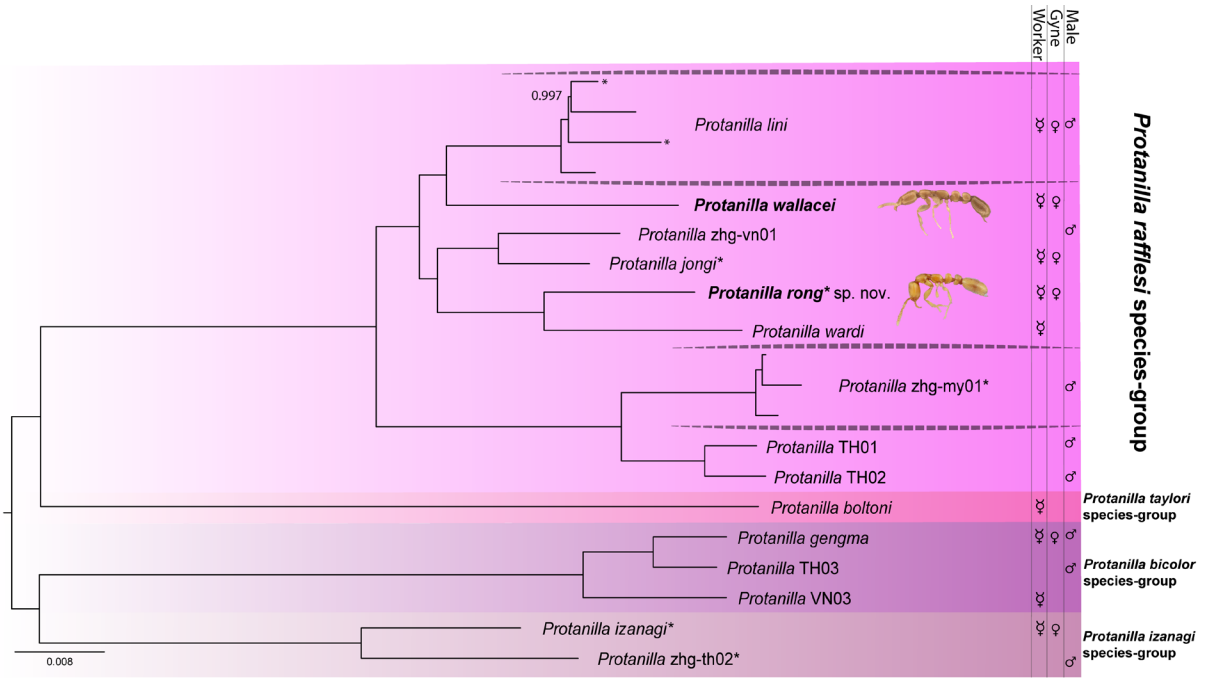

Fig. 1. Phylogeny of *Protanilla* Taylor, 1990, as inferred in ExaBayes ver. 1.4.1 from 534 UCE loci trimmed with lognormal threshold = 0.90 in Spruceup. Outgroups not shown; terminals novel to this study are shown with an asterisk. Scale bar is expressed in number of expected substitutions per site, and BPP = 1 for nodes unless otherwise noted. If multiple exemplars of a putative species were included, these are delimited from other specimens by asymmetrical dotted lines. Worker representatives of *Protanilla wallacei* Griebenow, 2024 and *Protanilla rong* sp. nov. are shown in profile view. Forms known for each putative species are plotted on the right.

inferences present no compelling evidence for the monophyly of *Protanilla* exclusive of the *Protanilla taylori* species-group. *Protanilla jongi* Hsu *et al.*, 2017 is revealed to belong well within the *Protanilla rafflesi* species-group, indirectly confirming the synonymy of *Furcotanilla* with *Protanilla* (Hsu *et al.* 2017; cf. Griebenow 2024: 123). *Leptanilla thai* Baroni Urbani, 1977 and *Leptanilla belantanoides* sp. nov. are recovered well within the former genus *Yavnella* Kugler. 1987 (i.e., the *Leptanilla thai* species-group; Griebenow 2024), while *Leptanilla havilandi* Forel, 1901 is found to be sister to the former genus *Noonilla* Petersen, 1968 (the *Leptanilla havilandi* species-group, in part; Griebenow 2024).

Protanilla rong sp. nov. is robustly recovered in all analyses as a closer relative of *P. jongi* than *Protanilla wallacei* Griebenow, 2024 despite closely resembling the latter (Fig. 1). Since there is no evidence to doubt the heterospecificity of *P. jongi* with *P. rong* or other relatives within the *Protanilla rafflesi* species-group, this phylogenomic result supports the validity of *P. rong* as a distinct species.

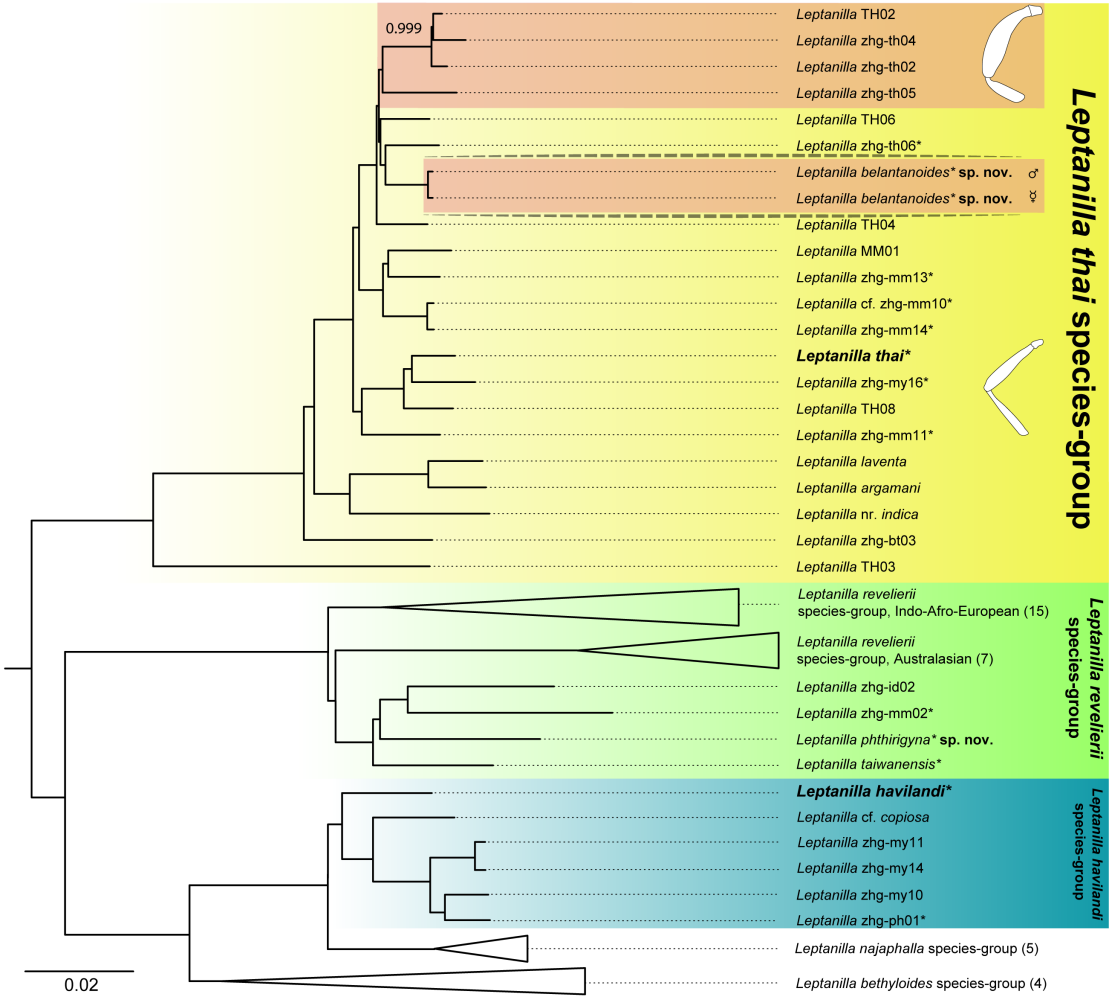

Fig. 2. Phylogeny of *Leptanilla*, as inferred in ExaBayes ver. 1.4.1 from 534 UCE loci trimmed with lognormal threshold = 0.90 in Spruceup. Scale bar is expressed in number of expected substitutions per site, and BPP = 1 for all shown nodes unless otherwise noted. Outgroup terminals are not shown, and the number of terminals in each collapsed clade is provided parenthetically. If multiple exemplars of a putative species were included, these are delimited from other specimens by asymmetrical dotted lines. Line drawings of the male foreleg in the *Leptanilla thai* species-group indicate its condition across that clade; orange boxes represent lineages with the derived condition. Asterisks mark terminals that are novel to this study.

The workers and putative male of *Leptanilla belantanoides* sp. nov. were collected 13 km apart, with respectively sequenced specimens of each recovered as close kin by phylogenomic inference with maximal support (Fig. 2), much as in the scenario of worker and male specimens of *Protanilla lini* Terayama, 2009 definitively associated by these same inferential methods (Griebenow 2020). It must be cautioned that this does not confirm the identity of the male as *L. belantanoides* sp. nov. with total certainty (see Discussion).

µ-CT of Leptanilla crania

In both *Leptanilla belantanoides* sp. nov. and *Leptanilla charonea*, the musculus clypeopalatalis (0ci1) has two components, one originating at the anteriormost margin of the clypeus, and one posterad to that. The anterior portion inserts on a finger-like projection of the dorsal wall of the sucking pump, while the posterior portion inserts around and posterad this projection. Musculus clypeobuccalis (0bu1) originates

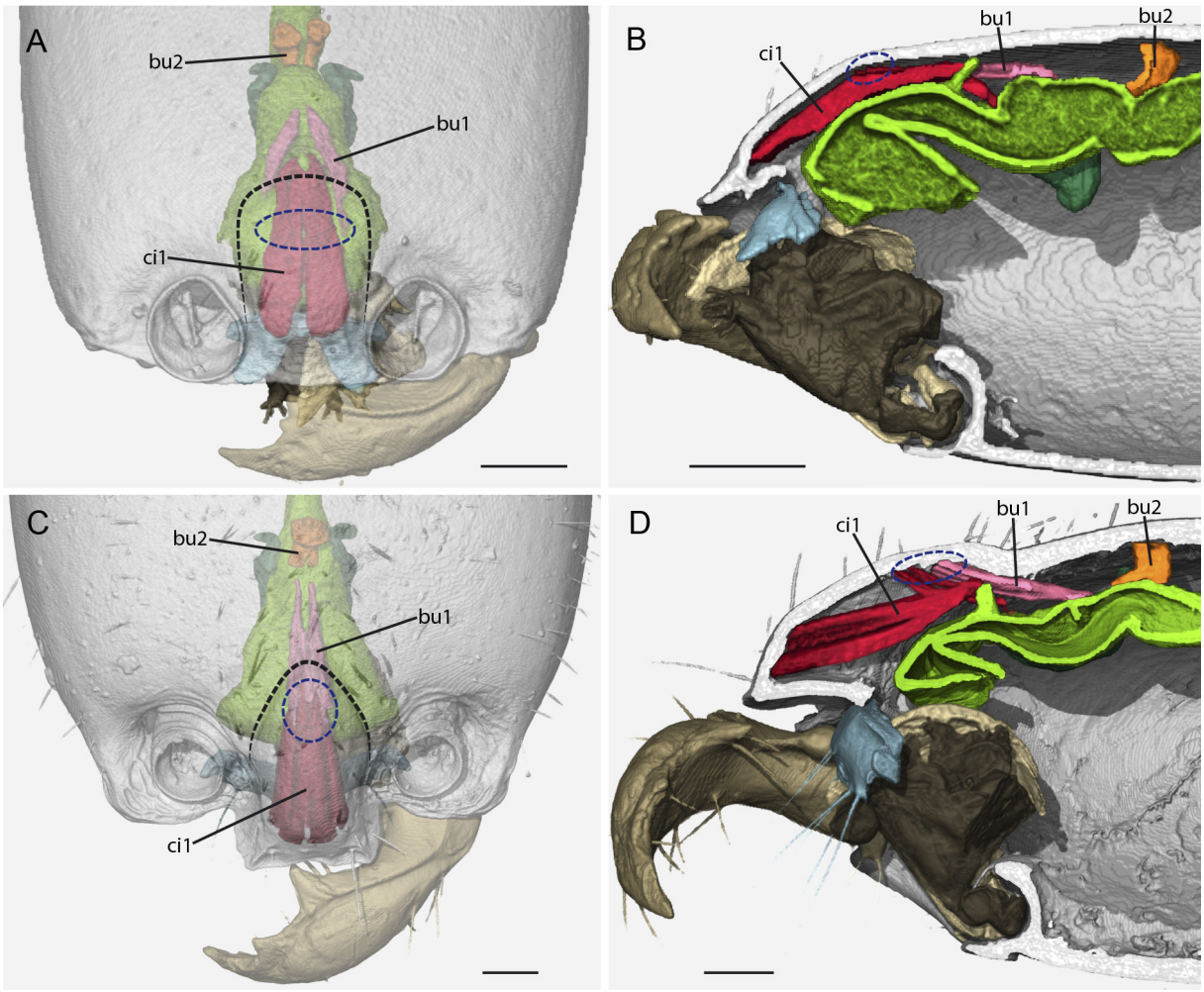

Fig. 3. Volume renderings of *Leptanilla* Emery, 1870 crania, focusing on the cephalic sucking pump (green) and clypeofrontal muscles (red, orange). Dotted lines delimit frons from clypeus, with blue dotted ovals marking relevant muscle origins. Infrabuccal pouch and epipharynx connecting the pump to the mouthparts not shown. **A**. *Leptanilla charonea* López, Martínez & Barandica, 1994, dorsal view. **B**. *L. charonea*, sagittal cross-section. **C**. *L. belantanoides* sp. nov., dorsal view. **D**. *L. belantanoides*, sagittal cross-section. Abbreviations: ci1 = Musculus (M.) clypeopalatalis; bu1 = M. clypeobuccalis; bu2 = M. frontobuccalis anterior. Scale bars = 0.03 mm.

immediately behind the posterior portion of 0ci1 in *L. belantanoides*, and laterad to 0ci1 in *L. charonea*. The origins of 0ci1 and 0bu1 together signify the posterior margin of the clypeus in these specimens (Snodgrass 1935).

Taxonomy

Class Insecta Linnaeus, 1758
Order Hymenoptera Linnaeus, 1758
Family Formicidae Latreille, 1802
Subfamily Leptanillinae Emery, 1910
Tribe Leptanillini Emery, 1910

Genus ***Protanilla*** Taylor, 1990

Protanilla Taylor in Bolton, 1990: 279, figs 1–6.
Anomalomyrma Taylor in Bolton, 1990: 278, fig. 8. Synonymy by Griebenow (2024: 117).
Furcotanilla Xu, 2012: 481, figs 9–12. Synonymy by Hsu *et al.* (2017: 119).

Diagnosis

Worker

Medial mandibular margin with regularly spaced denticles; ventromedial teeth present or absent. Labrum with multiple rows of peg- or pencil-like chaetae (Griebenow 2024: figs 4c, 21a–b). Palp formula 4,1-3. Clypeus distinct; epistomal sulcus present. Pair of medial chaetae on second protarsomere. Meso-metapleural suture present, scrobiculate. Cuticular microsculpture absent from most sclerites; if present, irregularly reticulate to rugose.

Gyne

As in worker, but alate.

Male

Palp formula 4,1-3. Ocelli present; not set on tubercle. Notauli present or absent. Pterostigma present. Upper metapleuron distinct from metapectal-propodeal complex; lower metapleuron indistinct from metapectal-propodeal complex. Cupula present, annular (cf. Griebenow *et al.* 2023: 957, fig. 4a–c, e) or not (Griebenow *et al.* 2023: fig. 4d). Volsellae present; parossiculus and lateropenite distinct. Penial sclerites medially articulated.

Global key to workers of *Protanilla*

Condensed and amended from Griebenow (2024: 150–152).

1. Abdominal tergite II without distinct posterior face (Griebenow 2024: fig. 34c); peg-like chaetae absent from mandible (*Protanilla taylori* species-group) 2
– Abdominal tergite II with distinct posterior face (Griebenow 2024: fig. 34b); peg-like chaetae present on mandible 3

2. Cranium, pronotum and mesopleuron puncticulate to roughly sculptured; subpetiolar process lacking fenestra in profile view .....***Protanilla boltoni*** (Borowiec *et al*., 2011) (MALAYSIA: Perak)
– Cranium, pronotum and mesopleuron glabrous; subpetiolar process with fenestra in profile view.... .....***Protanilla helenae*** (Borowiec *et al*., 2011) (PHILIPPINES: Palawan)

3. Clypeus oblate-trapezoidal in outline, elevated above frons posteriorly (Griebenow 2024: fig. 35a); mandible bowed along anteroposterior axis of cranium (*Protanilla izanagi* species-group) ..... ***Protanilla izanagi*** Terayama, 2013 (JAPAN: Honshu)
– Clypeus campaniform in outline, not elevated above frons posteriorly (Fig. 11C); mandible straight 4

4. Mesotibia with one spur; mandible without laterodorsal longitudinal groove; anterior margin of clypeus concave (*Protanilla bicolor* species-group) 5
– Mesotibia without spurs; mandible with laterodorsal longitudinal groove; anterior margin of clypeus planar (*Protanilla rafflesi* species-group) 6

5. Cranium black-brown; anterior face of petiolar node sloping in profile view ..... ***Protanilla gengma*** Xu, 2012 (CHINA: Yunnan; INDIA: Mizoram; VIETNAM: Dong Nai, Bac Giang, Ninh Binh)
– Cranium yellowish; anterior face of petiolar node subvertical in profile view ..... ***Protanilla bicolor*** Xu, 2002 (CHINA: Yunnan)

6. Abdominal sternite III linear to slightly concave in profile view; abdominal segments III–IV broadly conjoined, with abdominal tergite III lacking a distinct posterior face 7
– Abdominal sternite III convex in profile view; abdominal segments III–IV not broadly conjoined, with abdominal tergite III having a distinct posterior face 8

7. Anterior margin of abdominal tergite IV emarginate in dorsal view; two ventrolateral teeth present on mandible ..... ***Protanilla furcomandibula*** Xu & Zhang, 2002 (CHINA: Yunnan)
– Anterior margin of abdominal tergite IV entire in dorsal view; one ventrolateral tooth present on mandible ..... ***Protanilla jongi*** Hsu *et al*., 2017 (TAIWAN)

8. Anterior face of petiolar node concave in profile view 9
– Anterior face of petiolar node linear in profile view 10

9. In profile view anterodorsal corner of petiolar node projecting anteriorly; larger species (WL > 0.8 mm) ..... ***Protanilla rafflesi*** Taylor, 1990 (SINGAPORE; MALAYSIA: Sabah, Sarawak)
– In profile view anterodorsal corner of petiolar node not projecting anteriorly; smaller species (WL = 0.70–0.80 mm) (n = 2) ..... ***Protanilla wardi*** Bharti & Akbar, 2015 (INDIA: Kerala)

10. In dorsal view petiolar node breadth and length subequal; postpetiolar node not inclined anteriorly in profile view 11
– In dorsal view petiolar node distinctly broader than long; postpetiolar node inclined anteriorly in profile view 15

11. Coloration castaneous (Griebenow 2024: fig. 22a); larger species (HL = 0.63–0.70 mm; WL = 0.99 mm) (n = 1) ..... ***Protanilla beijingensis*** Man *et al*., 2017 (CHINA: Beijing; PAKISTAN: Khyber Pakhtunkhwa)
– Coloration coppery or yellowish; smaller species (HL = 0.42–0.59 mm; WL = 0.61–0.94 mm) (n = 16) 12

12. Scape not extending beyond occipital vertex of cranium in full-face view (SI ≤ 90); coloration coppery ..... ***Protanilla flamma*** Baidya & Bagchi, 2020 (INDIA: Goa)
– Scape extending beyond occipital vertex of cranium in full-face view (SI > 90); coloration yellowish (Griebenow 2024: fig. 4a–c) 13

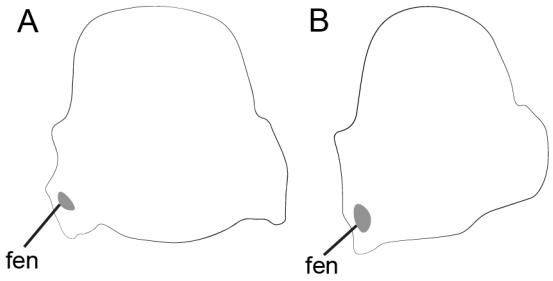

Fig. 4. Profile of abdominal segment II, diagrammatic. **A**. *Protanilla wallacei* Griebenow, 2024. **B**. *Protanilla rong* sp. nov. Abbreviation: fen = subpetiolar fenestra.

13. Larger species (WL≥0.75 mm) (n = 14); postpetiolar node prominent in profile view, with anterior and posterior declivities equally rounded (Griebenow 2024: fig. 6a) .... ***Protanilla lini*** Terayama, 2009 (TAIWAN; CHINA: Hong Kong; JAPAN: Okinawa, Ryukyu Islands; Senkaku Islands)
– Smaller species (WL<0.75 mm) (n = 11); postpetiolar node shallow in profile view, with posterior declivity more gradual than anterior declivity (Griebenow 2024: fig. 5a) 14

14. Dorsal mandibular articulation obtuse; subpetiolar process not extending ventrad remainder of abdominal sternite II (Fig. 4A) .... ***Protanilla wallacei*** Griebenow, 2024 (MALAYSIA: Sabah, Selangor)
– Dorsal mandibular articulation acute; subpetiolar process extending ventrad remainder of abdominal sternite II (Fig. 4B) .....***Protanilla rong*** sp. nov. (VIETNAM: Ninh Binh)

15. Lateral margin of head with acute dorsal mandibular articulation in full-face view; anteroventral corner of sub-post-petiolar process obliquely truncated ....***Protanilla tibeta*** Xu, 2012 (CHINA: Xizang)
– Lateral margin of head without dorsal mandibular articulation apparent in full-face view (Griebenow 2024: fig. 24a); anteroventral corner of sub-post-petiolar process rounded 16

16. Meso-metapleural furrow deeply excavated in profile view; very large species (HW = 0.82–0.84 mm) (n = 3) (Satria *et al.* 2023) ..... ***Protanilla eguchii*** Satria *et al*., 2023 (INDONESIA: Sumatra)
– Meso-metapleural furrow shallowly excavated in profile view; smaller species (HW = 0.48 mm) (n = 1) .....***Protanilla concolor*** Xu, 2002 (CHINA: Yunnan)

Protanilla gengma Xu, 2012
Figs 5–10

Protanilla gengma Xu, 2012: 485–486, figs 13–16.

Diagnosis

Worker

Cranium dark, conspicuously narrowed anteriorly. Mandible sublinear, with medial peg-like chaetae; dorsal lamella absent; laterodorsal longitudinal groove absent. Outline of clypeus campaniform, surface anteriorly concave; median clypeal ridge not visible. In dorsal view, PrW subequal to propodeal breadth. Mesotibia with one spur. Petiole sessile; anterior corner of dorsal petiolar node rounded in profile view; subpetiolar fenestra present. Abdominal segments II–III without tergotergal and sternosternal fusion; abdominal sternite III convex in profile view. Abdominal segments III–IV narrowly joined; anterior margin of abdominal tergite IV slightly emarginate in dorsal view.

Gyne

As for worker, but with compound eye.

Male

Distal 3 maxillary palpomeres subequal in length. Labial palp 2–3-merous. LF2 ≈ SL. Notauli present, scrobiculate. Hindwing 1A spectral to absent. Abdominal segment III petiolate. Length of abdominal postsclerites IV> combined length of abdominal postsclerites V–VIII. Cupula annular. Ventral penial process present.

Material examined

VIETNAM – **Ninh Binh** • 4 workers; Cuc Phuong National Park; 20.3496° N, 105.5957° E; 400 m a.s.l.; 8 Aug. 2022; M.G. Branstetter leg.; #4340; IEBR • 1 gyne; same data as for preceding; IEBR, CASENT0842884 • 30 larvae; same data as for preceding; IEBR, CSUENT6000161. – **Bac Giang** • 2 ♂♂; Tay Yen Tu Nature Reserve; 21.1792° N, 106.7228° E; 238 m a.s.l.; 30 Mar. 2003; K. Eguchi leg.; in rotten wood; Katsuyuki Eguchi personal collection, CSUENT6000018, CSUENT6000019 • 1 worker; same data as for preceding; CSUENT6000048 • 1 gyne; same data as for preceding; CSUENT6000047 • 1 worker; Tay Yen Tu Nature Reserve; 21.1697° N, 106.7183° E; 435 m a.s.l.; 27 May 2004; K. Eguchi leg.; Katsuyuki Eguchi personal collection, CASENT0179564.

Measurements and indices

Worker (n = 5)

HW = 0.46–0.49 mm; HL = 0.55–0.58 mm; SL = 0.48–0.52 mm; ML = 0.28–0.39 mm; WL = 0.91–0.95 mm; PrW = 0.38–0.40 mm; MW = 0.27–0.29 mm; PTL = 0.29–0.35 mm; PTH = 0.38–0.39 mm; PTW = 0.21–0.23 mm; PPL = 0.26–0.30 mm; PPW = 0.25–0.27 mm; PPH = 0.39–0.40 mm; CI = 83–85; SI = 99–110; MI = 60–79; PI = 63–77; PPI = 86–95.

Gyne (n = 2)

HW = 0.53–0.55 mm; HL = 0.63–0.64 mm; EL = 0.05–0.06 mm; EW = 0.04 mm; SL = 0.53–0.56 mm; ML = 0.32–0.38 mm; WL = 1.05–1.07 mm; PrW = 0.45–0.46 mm; MW = 0.32–0.33 mm; PTL = 0.32–0.36 mm; PTH (n = 1) = 0.45 mm; PTW = 0.27 mm; PPL = 0.28–0.30 mm; PPW = 0.30–0.35 mm; PPH = 0.46–0.47 mm; CI = 84–87; SI = 96–105 mm; MI = 61–69 mm; REL = 8–10; OI = 61–85; PI = 75–84; PPI = 108–118.

Male (n = 2)

HW = 0.64–0.65 mm; HL = 0.50–0.51 mm; EL = 0.27–0.28 mm; EW = 0.20–0.21 mm; SL = 0.17–0.18 mm; LF2 = 0.16 mm; MaL = 0.06 mm; WL = 1.06–1.11 mm; PrW = 0.56–0.57 mm; MSW = 0.51–0.58 mm; MSL = 0.54–0.55 mm; PTL = 0.22–0.23 mm; PTH = 0.20–0.22 mm; PTW = 0.18–0.19 mm; PPL = 0.22 mm; PPW = 0.24 mm; PPH = 0.25–0.27 mm; TW4 (n = 1) = 0.58 mm; CI = 124–132; SI = 27–28; MI = 16–17; OI = 74–75; REL = 53–57; MSI = 94–95; PI = 79–87; PPI = 107–113; TI1 (n = 1) = 46.

Description

Male

Head in full-face view suboval, wider than long (CI = 124–132); occiput entire. Mandibles reduced, nub-like, edentate, articulated to cranium; mandalus large, occupying most of anterior half of mandibular dorsal surface. Labrum reduced. Palpal formula 4,3. Maxillary palpomeres II–IV elongate, each longer than maxillary palpomere I. Labial palpomeres II–III ~0.5× respective lengths of maxillary palpomeres II–III, respectively. Median clypeal length approximately 1.4 × torular diameter; anterior margin weakly medially concave; posterior margin slightly produced between toruli. Anterior tentorial pit directly anterad antennal torulus in full-face view. Ocellar tubercle absent. Occipital carina present only dorsally.

Compound eyes large (REL = 53–57), oval; all margins weakly convex. Antenna 13-merous, filiform; scape cylindrical, SL < EL or EW; pedicel subcylindrical, length a little less than 0.5× SL; antennomere III nearly as long as scape (LF2 = 0.16 mm; SL 0.17–0.18 mm).

In lateral view, anterodorsal face of pronotum depressed at transition to pronotal flange. Mesoscutum strongly convex, slightly longer than height or lateromedian breadth. Antero-admedian signum present. Notauli present, meeting at posterior mesoscutal margin. Parapsidal signa present, weakly impressed, slightly divergent anteriorly. Scutoscutellar sulcus deep and broad. Oblique mesopleural sulcus broad,

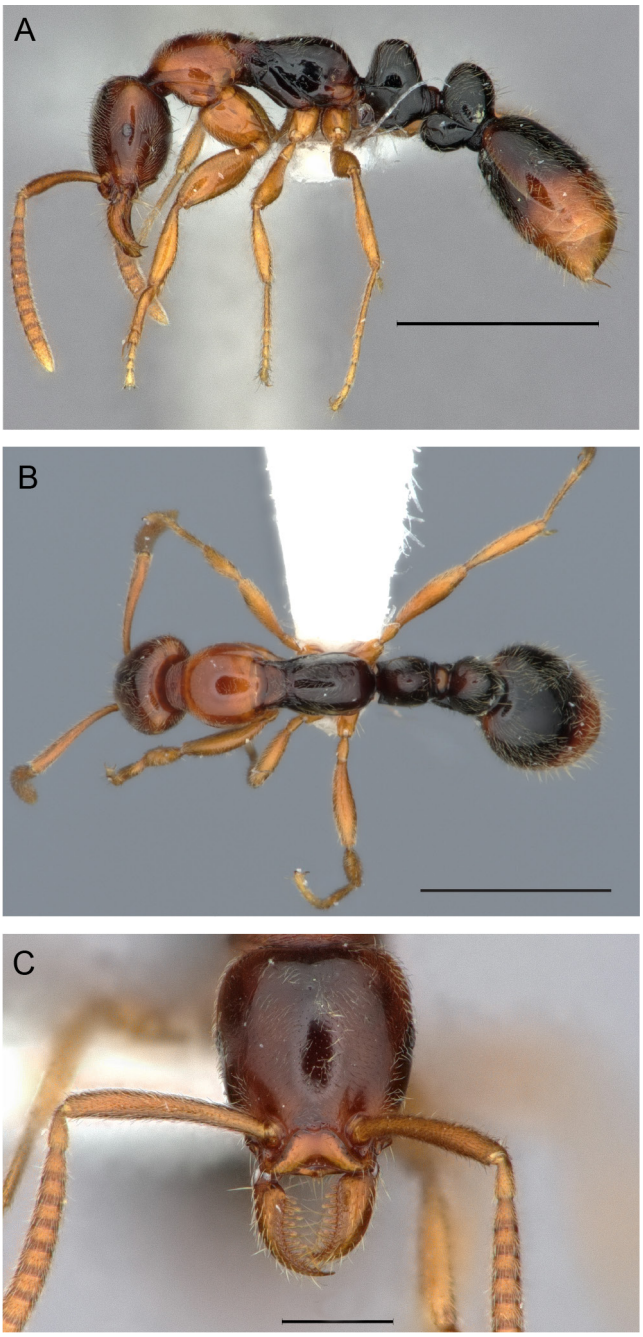

Fig. 5. *Protanilla gengma* Xu, 2012, gyne (CASENT0842884). **A**. Profile view. **B**. Dorsal view. **C**. Full-face view. Scale bars: A–B = 1 mm; C = 0.3 mm.

scrobiculate, bisecting mesopectus. Mesoscutellar height and length subequal, posterodorsal mesoscutellar face convex, not posteriorly produced in lateral view; mesoscutellar disc wider than long; mesoscutellar dorsum high as that of mesoscutum. Metanotum strongly convex in lateral view, with dorsal face narrowly visible in dorsal view. Metapleural gland absent. Propodeum convex in lateral view, without distinct dorsal face; propodeal lobe absent. All legs similar, trochanters sphenoid (i.e., wedge-shaped), femora straight and somewhat anteroposteriorly compressed; proximodistal length of protrochanters ~1.5× as great as width, meso- and metatrochanters ~2× as great as width. Tibial spur formula 1b,1p. Wing membranes hyaline. In forewing, C, Sc+R+Rs, Rf, Mf1, and 1A tubular; 2s-rs+Rs+4-6 spectral; M+Cu spectral; *cu-a* with weakening adjacent to 1A. Pterostigma present, large. Hindwing with R+Rs tubular, extending ¼ of distance along costal margin; 1A spectral, ~0.17× length of R+Rs.

Abdominal segments II–III petiolate, with complete tergosternal fusion and distinct tergosternal sutures. Abdominal segment II sessile, longer than wide (PI = 79–87), length and height subequal; lateral margins subparallel in dorsal view; abdominal tergite II convex, but petiole without dorsal node; in ventral view, abdominal tergite II subrectangular with rounded margins. Abdominal segment III wider than long (PPI = 107–113), 1.12–1.24× as high as long; post-tergite III weakly raised and convex posteriorly; abdominal poststernite III in lateral view with distinct rounded corner, outline of ventral margin sublinear. Abdominal segments IV–VIII without tergosternal fusion.

Spiculum present; abdominal sternite IX with robust posteromedian process. Cupula annular, lateromedial breadth slightly greater than maximum anteroposterior length; dorsum anteroposteriorly compressed. Gonopodites articulate. Gonocoxites with complete median fusion, with conspicuous sutures ("dgcs" and "vgcs" in Fig. 8C–D); gonocoxital arms fused to form anteromedian apodeme with acute apex, making ventral outline of gonocoxital foramen strongly emarginate in ventral view. Gonostylus a little shorter

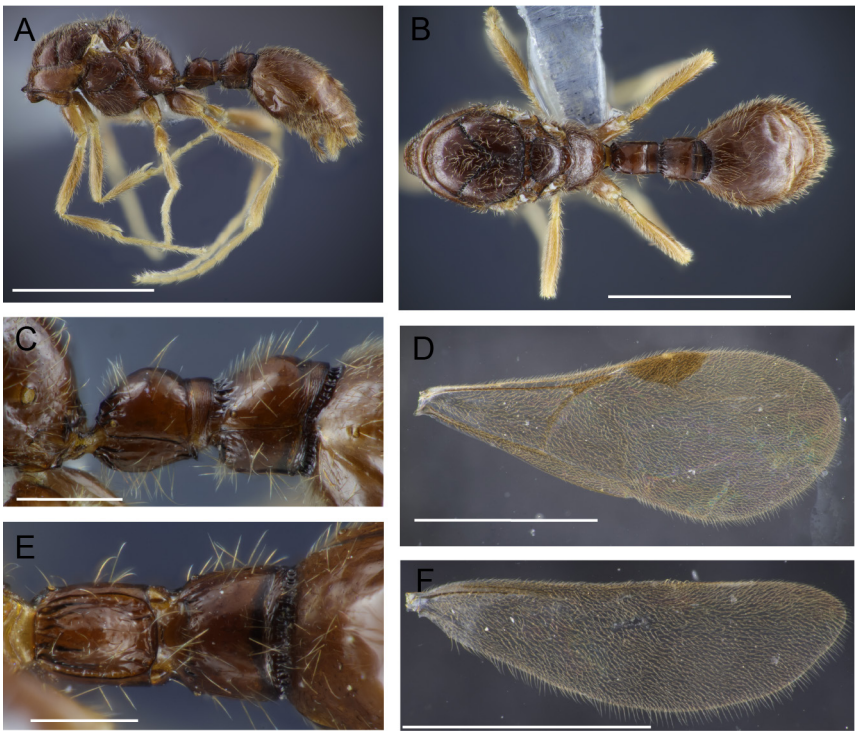

Fig. 6. *Protanilla gengma* Xu, 2012, male (CSUENT6000018). **A**. Profile view. **B**. Dorsal view. **C**. Abdominal segments II–III, profile view. **D**. Forewing. **E**. Abdominal segments II–III, ventral view. **F**. Hindwing. Scale bars; A–B, D, F = 1 mm; C, E = 0.2 mm.

than gonocoxite, slightly recurved medially in dorsal view. Parossiculus lateromedially compressed, about 0.5× as long as lateropenite; outline lobate in lateral view, with a few trichoid sensilla on apex. Lateropenite blunt, uncinate in lateral view, apex curved ventrad; ectal surface covered with dense

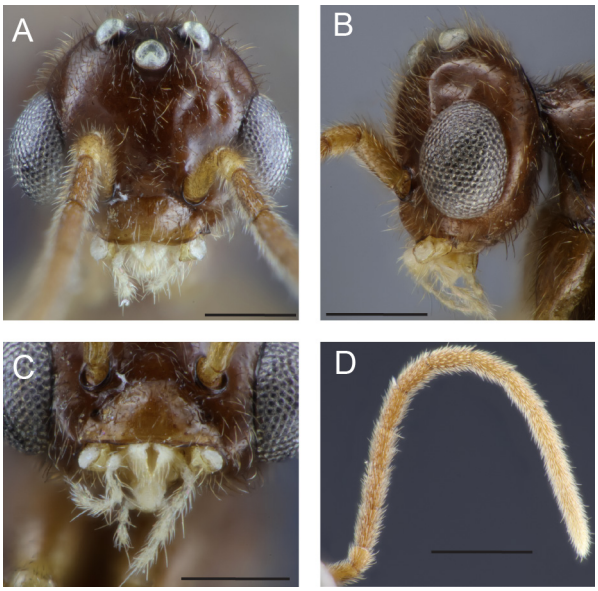

Fig. 7. *Protanilla gengma* Xu, 2012 (CSUENT6000019), male head. **A**. Full-face view. **B**. Profile. **C**. Mouthparts, anterior. **D**. Antenna. Scale bars: A–C = 0.2 mm; D = 0.5 mm.

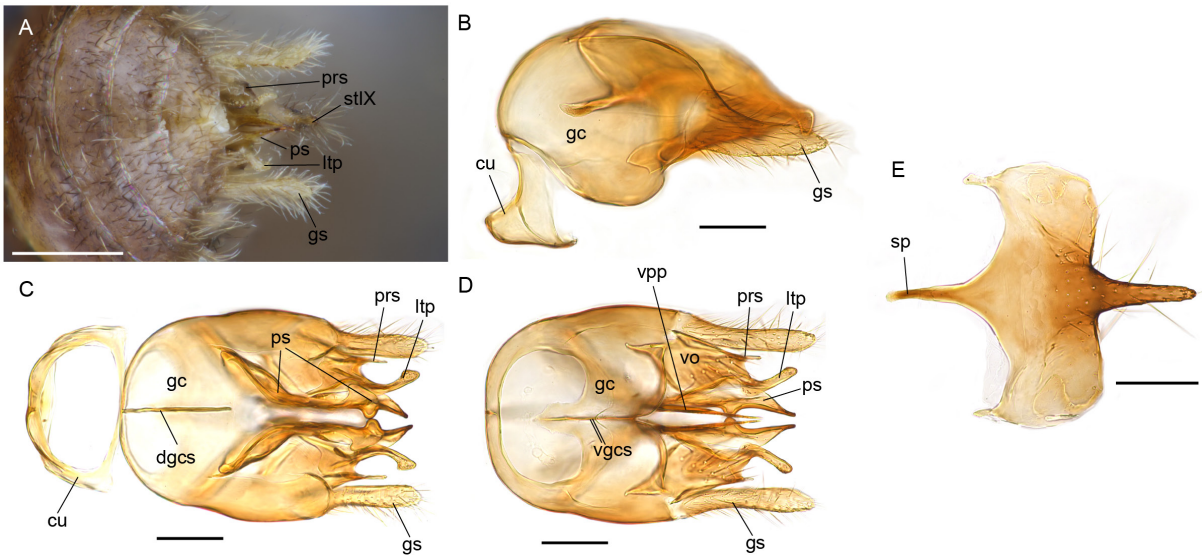

Fig. 8. *Protanilla gengma* Xu, 2012, male genitalia in situ (A; CSUENT6000018) and macerated (B–E; CSUENT6000019). **A**. Genitalia and abdominal tergites VI–VIII in situ, posterodorsal view. **B**. Genitalia, profile view. **C**. Genitalia, dorsal view. **D**. Genitalia, ventral view. **E**. Abdominal sternite IX. Abbreviations: cu = cupula; dgcs = dorsomedian gonocoxital suture; gc = gonocoxite; gs = gonostylus; ltp = lateropenite; prs = parossiculus; ps = penial sclerites; sp = spiculum; stIX = abdominal sternite IX; vgcs = ventromedian gonocoxital suture; vo = volsella; vpp = ventral penial process. Scale bars: A = 0.2 mm; B–E = 0.1 mm.

basiconic sensilla; ventromesal margin with conspicuous lateral flange (Fig. 9E; "ltpf"). Penial sclerites without medial fusion, connected via dorsomedial conjunctiva; proximodorsally fused with gonocoxites, but connection weakly sclerotized. Preapical dorsum of penial sclerite bears conspicuous rounded lobes, produced laterad and mesad respectively (Fig. 9F–G; "lpl", "mpl"); lateral lobe lamellate, relatively broad; mesal lobe thicker and narrower. Distodorsal part of penial sclerite smoothly tapering in lateral view, with downcurved apex subacute, ventral denticles absent. Proximoventral part of penial sclerite with long saw-like ventral process ("vpp" in Figs 8D, 9G) originating distal to lateral penial apodeme, produced ventrad and distad, recurved posterad at ~90° angle; in lateral view its distoventral and distodorsal margins bear ~ 58 small denticles; distal apex acute. Body dark brownish with paler antenna, mouthparts, and legs. Body sculpture mostly lacking; pronotal flange and anterior of abdominal postsclerites II–III coarsely longitudinally rugose; cinctus of abdominal segment IV scrobiculate. Somal pilosity as in Fig. 6.

Gyne

As for worker, completely lacking alar sclerites, but somewhat larger (WL = 1.05–1.07 mm) and with compound eye (Fig. 5B). Compound eye anteroposteriorly compressed, small (REL = 10), with 12 ommatidia.

Supplementary description

Worker

As in Xu (2012: 485–486), but with the following additions or differences. Labrum with three chaetae. Two rows of mandibular chaetae present, with 12 in dorsal row and 9 in ventral row; ventral row with

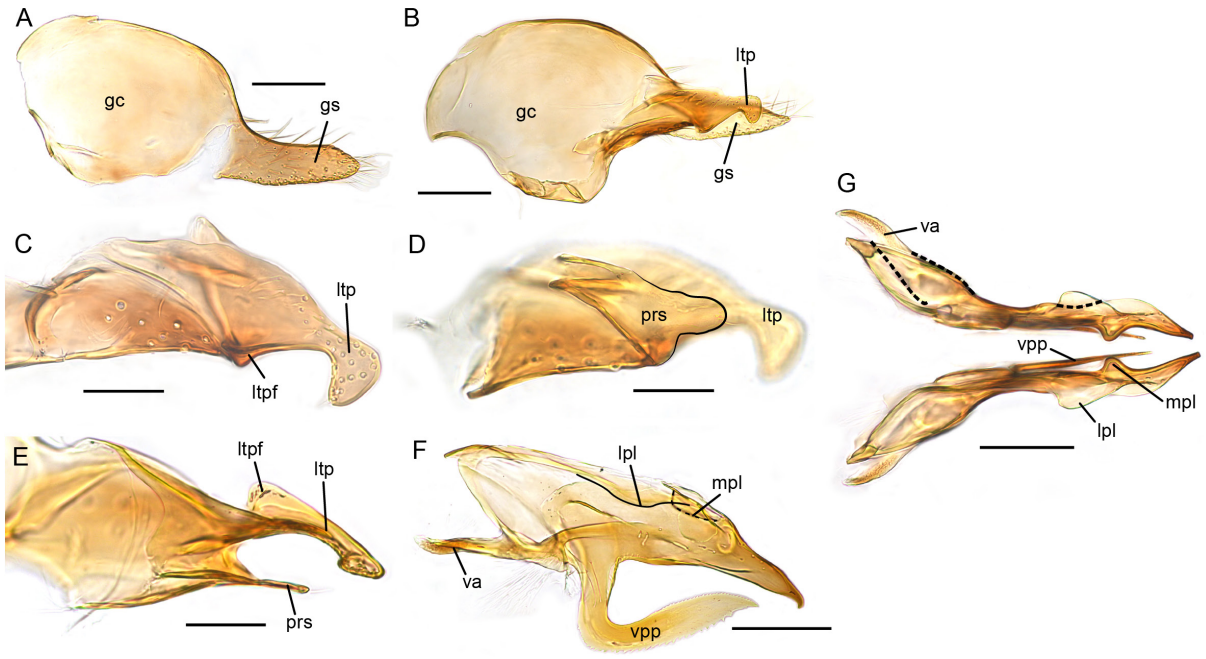

Fig. 9. Male genitalia of *Protanilla gengma* Xu, 2012, macerated. **A–B, G**. Specimen CSUENT6000018. **C–F**. Specimen CSUENT6000019. **A**. Gonopodite, ectal profile view. **B**. Gonopodite and volsella, mesal profile view. **C**. Volsella, mesal view. **D**. Volsella, ectal view. **E**. Volsella, dorsal view. **F**. Penial sclerite, mesal view. **G**. Penial sclerites, dorsal view. Abbreviations: gc = gonocoxites; gs = gonostylus; lpl = lateral penial lobe; ltp = lateropenite; ltpf = ventromesal lateropenital flange; mpl = mesal penial lobe; prs = parossiculus; va = valvura; vpp = ventral penial process. Scale bars: A–B, F–G = 0.1 mm; C–E = 0.05 mm.

chaetae expanded distally, except for most proximal chaeta. Subapical mandibular seta present. Palp formula 4,3. Tibial spur formula 1p,1p.

Distribution

Further sampling is needed across the putative range of *P. gengma* to establish the scope of intraspecific variation. The specimens from Cuc Phuong National Park differ from the holotype in having three labral chaetae rather than four, as in the population of *P. gengma* reported from Mizoram, India (Aswaj *et al.* 2020). This and other differences between the holotype and the specimens reported here, along with those collected in Mizoram, are of unclear significance for species delimitation. The male of *P. gengma* closely resembles that of *Protanilla* TH03, with the only apparent difference being palpomere count and coloration, with *Protanilla* TH03 blackish, whereas *P. gengma* is browner; this variation may be intraspecific.

Ecology

The collections of *Protanilla gengma* reported here from Tay Yen Tu Nature Preserve are the first from rotten wood, rather than soil or leaf litter (Xu 2012; Aswaj *et al.* 2020). A pharate worker is here reported within a cocoon from collection #4340 at Cuc Phuong National Park, marking the first such record for *Protanilla* (Fig. 10A). This collection also contained 28 larvae feeding on a juvenile scolopendromorph centipede, consistent with behavior observed in other Leptanillinae. All larvae attached to the centipede were identical in size, therefore appearing to be in the same instar. The co-occurrence of a pharate adult and at least two larval instars would seem to argue against synchronous brood production in *P. gengma*.

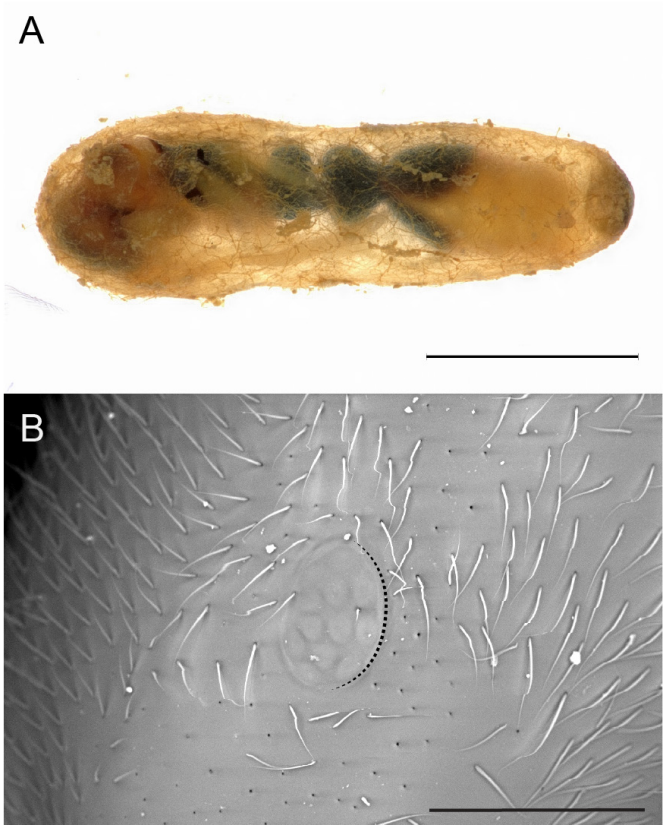

Fig. 10. Attributes of *Protanilla gengma* Xu, 2012. **A**. Pharate worker enclosed in cocoon. **B**. Gyne of *Protanilla gengma* (CASENT0842884), profile view of cranium; compound eye indicated posteriorly by dotted line. Scale bars: A = 0.5 mm; B = 0.01 mm.

Remarks

The contents of Eg03-VN-106 were reported by Eguchi *et al.* (2014: 23, figs 7–8) as *Protanilla* sp. eg-1, while CASENT0179564 was provisionally referred to as *Protanilla* VN01 in preceding literature (Borowiec *et al.* 2019; Griebenow 2020; Griebenow *et al.* 2022). The 3-merous labial palp of both worker and male is exceptional among the Leptanillinae, amending the diagnosis for *Protanilla* and Leptanillinae for both forms. A 2-merous labial palp is implied to be an apomorphy of the Opamyrmini and *Leptanilla*. Without reexamination of *Protanilla* TH03 we cannot confirm that the assessment of the labial palp as 2-merous in this male morphospecies (Griebenow 2020: fig. 10b) was accurate.

The description of the first known male belonging to the *Protanilla bicolor* species-group notably reveals an annular cupula, contrasting with the non-annular cupula of the *Protanilla rafflesi* species-group (Griebenow *et al.* 2023) and *Opamyrma* (Yamada *et al.* 2020). The annular cupula of *Protanilla gengma*, and its anterior separation from abdominal sternite VIII–IX and the gonocoxites, is a symplesiomorphy with at least one representative of the *Leptanilla thai* species-group (*Leptanilla* zhg-bt03) and the *Leptanilla bethyloides* species-group (Griebenow *et al.* 2023).

The ergatogyne here described is the first reproductive female documented for the *Protanilla bicolor* species-group. Unlike the ergatogynes known in at least one species of the *Protanilla rafflesi* species-group (Ito *et al.* 2022), alar sclerites are completely lacking in the ergatogyne of *P. gengma*. Most *Protanilla* gynes are alate, indicating that aptery in female reproductives has evolved at least twice in *Protanilla*, and moreover in different subclades.

Protanilla rong sp. nov.
urn:lsid:zoobank.org:act:548AA897-78C9-4D5E-911B-EBEBA3721404
Figs 11–13

Surface mesh of gyne: https://sketchfab.com/3d-models/casent0745747-protanilla-rong-queen-9c0c45b9ece544bb96cba5518c8762c1
Surface mesh of worker: https://sketchfab.com/3d-models/casent0745809-protanilla-rong-worker-7349bc16ae7d4520a9f5395e29c0cd0f
Surface mesh of larva: https://sketchfab.com/3d-models/casent0745741-protanilla-rong-larva-83ab874c2fa8426ab1f43d33872e0125

Diagnosis

Worker

Lateral cranial margins converging anteriorly; cranium not bulging towards vertex. Dorsal mandibular articulation visible in full-face view, acute. Clypeal surface planar, posteriorly not elevated above frons; posteromedian margin entire; median clypeal ridge present, visible externally; outline campaniform. Labrum armed with three peg-like chaetae. Mandible linear, without vertical dorsal lamella or laterodorsal longitudinal groove; dorsomedial margin with single row of ~12 peg-like chaetae; lateral mandibular face glabrous. Labial palp 1-merous. Meso- and metatibial spur formula 0,1p. Petiole sessile, with dorsal node having distinct posterior face; anterior face linear in profile view. In dorsal view, length and breadth of petiolar node subequal. Subpetiolar process present, projecting ventrad the remainder of ventral margin of abdominal sternite II; abdominal sternite II with margin not concave posterad subpetiolar process; fenestra present. Abdominal segments II–III without tergotergal and sternosternal fusion. Dorsal node of abdominal segment III with distinct posterior face, gently sloping. Abdominal segments III–IV not broadly conjoined. Soma concolorous, color yellowish.

Etymology

From the Vietnamese "rồng", meaning "dragon". The Vietnamese conception of a dragon is tubular and sinuous, with short legs, and often golden coloration. This habitus recalls the Leptanillinae, and

particularly the deep yellow color of *Protanilla rong* sp. nov. The specific epithet is a noun in apposition, and therefore invariant.

Type material

Holotype

VIETNAM – **Ninh Binh** • worker; Cuc Phuong National Park, 350 m NW of park headquarters, 1–2 cm within macrotermitine mound; 20.253° N, 105.217° E ± 200 m; 145 ± 5 m a.s.l.; 10 Aug. 2022; A. Richter leg.; IEBR, CASENT0842870.

Paratypes

VIETNAM – **Ninh Binh** • 7 workers; same data as for holotype; IEBR, CASENT0842862, CASENT0842871 to CASENT0842874, CASENT0842876, CASENT0842877 • 1 gyne; same data as for holotype; IEBR, CASENT0745747.

Other material examined

VIETNAM – **Ninh Binh** • 1 larva; same data as for preceding; IEBR, CASENT0745741.

Measurements and indices

Holotype

HW = 0.36 mm; HL = 0.47 mm; SL = 0.35 mm; ML = 0.25 mm; WL = 0.66 mm; PrW = 0.27 mm; MW = 0.20 mm; PTL = 0.20 mm; PTH = 0.26 mm; PTW = 0.17 mm; PPL = 0.18 mm; PPW = 0.20 mm; PPH = 0.25; CI = 76; SI = 100; MI = 70; PI = 88; PPI = 112.

Paratype workers

HW = 0.35–0.37 mm; HL = 0.43–0.47 mm; SL = 0.34–0.37 mm; ML = 0.23–0.25 mm; WL = 0.62–0.66 mm; PrW = 0.24–0.28 mm; MW = 0.19–0.20 mm; PTL = 0.17–0.20 mm; PTH = 0.24–0.27 mm; PTW = 0.16–0.19 mm; PPL = 0.17–0.18 mm; PPW = 0.19–0.20 mm; PPH = 0.24–0.26 mm; CI = 76–82; SI = 97–101; MI = 65–70; PI (n = 6) = 82–99 mm.

Paratype gyne

HW = 0.42 mm; HL = 0.50 mm; EL = 0.10 mm; EW = 0.10 mm; SL = 0.38 mm; ML = 0.31 mm; PrW = 0.32 mm; WL = 0.86 mm; MW = 0.29 mm; PTL = 0.19 mm; PTH = 0.33 mm; PTW = 0.22 mm; PPL = 0.20 mm; PPW = 0.24 mm; PPH = 0.32 mm; CI = 78; SI = 98; MI = 79; REL = 20; OI = 100; PI = 118; PPI = 123.

Description

Worker

As for *Protanilla wallacei* (Griebenow 2024: 91–93), but dorsal mandibular articulation acute in full-face view. Posteromedian clypeal margin entire. Anterior of labrum armed with three dentiform, peg-like chaetae. Abdominal sternite II with margin sinuate in profile view, not concave posterad subpetiolar process; subpetiolar process projecting ventrad the remainder of ventral margin of abdominal sternite II; fenestra present, elliptical, not anteroposteriorly compressed, occupying whole of subpetiolar process. Color yellowish.

Gyne

Head longer than wide (CI = 84); lateral margins moderately convex; occiput emarginate. Compound eyes located slightly behind head midline. Ocelli present. Clypeus as in worker. Labrum visible in full face view; bearing one central, dentiform, peg-like chaeta and a pair of longer, straight setae below it; more distal surface of labrum covered in long, suberect setae, with a short pair of setae centrally. Mandible shape as in workers; mesal margin of mandible with rounded denticles proximally, denticles flattening towards apex; downcurved mandibular apex with three larger denticles; mesal margin

proximad mandibular apex with row of 12 dentiform, peg-like chaetae, ventrad denticles; only few long setae inserted below chaetae, longest seta on inner side of apical tooth; outer mandibular surface covered sparsely in setae. Palp formula as in worker; proximal labial palpomere very short, hidden below labrum. Anterior tentorial pit indistinct, laterad and very close to antennal torulus. Postgenal ridge complete. Antenna as in worker. Alar sclerites present, but specimen dealate. Pronotum in dorsal view approximately as long and wide as scutum, with convex sides; outline convex in lateral view.

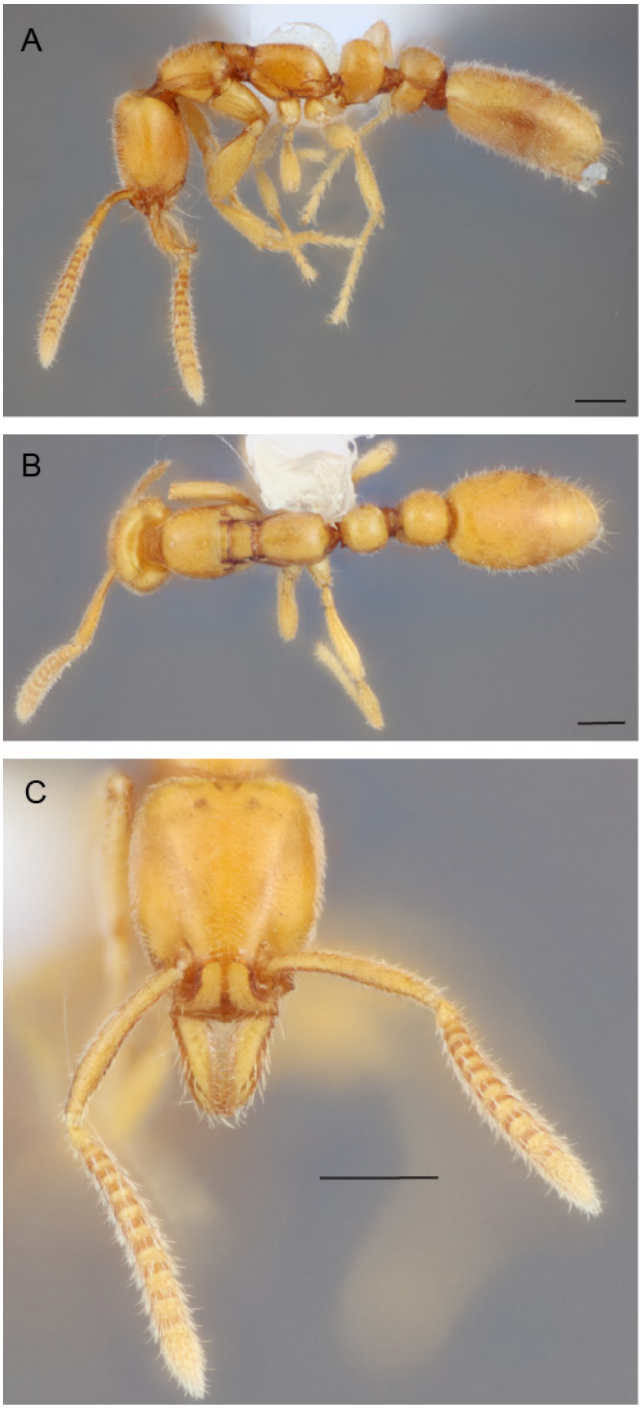

Fig. 11. *Protanilla rong* sp. nov., holotype, worker (CASENT0842870). **A**. Profile view. **B**. Dorsal view. **C**. Full-face view. Scale bars: A–B = 0.2 mm; C = 0.25 mm.

Mesoscutum a rounded trapezoid in dorsal view, slightly convex in profile view. Mesoscutellum in dorsal view <0.5× mesoscutal length, slightly convex in profile view. Mesopleural area in profile view wide, with narrow meso-metapleural suture. Propodeal width in dorsal view subequal to mesoscutal width, slightly narrowing posteriorly; outline convex in lateral view. Bulla proportionally more elongate than in worker, extending anterad propodeal spiracle. Tibial spurs as in worker. Abdominal segment II about as long as wide in dorsal view (PI = 118); petiolar node anteroposteriorly compressed, with anterior face slightly concave in profile view. Anterior outline of subpetiolar process with backwards bent in distal quarter; posterior outline slightly concave in profile view; process appearing roughly triangular overall. Abdominal segment III proportionally shorter in profile view than in worker (PPI = 123). Coloration as in worker. Vestiture of short, suberect setae present, interspersed with slightly longer erect setae.

Larva

Instar uncertain. Stenocephalous, with abdominal segment XI widest. Cranium subcircular, almost globular in full-face view, surface smooth and glabrous. Antenna set slightly behind midline of cranium, in full face view as distant from other antenna medially as to lateral margin of cranium, consisting of two flat cone-shaped sensillae in small pits. Mandibles typhlomyrmecoid; ectal surface with a few rounded cuticular processes. Maxilla with two short setae laterally; maxillary palp stout, peg-like, with conical sensillum at apex, two sensillae on ectal surface proximad apex. Galea slightly narrower and longer than palp, with two short, peg-like apical setae. Labrum indistinctly separated from cranium; labral margin with four flat, conical sensilla, and row of minute cuticular projections. Labium with comb of thick microtrichia on a rectangular, shelf-like projection distally, likely representing the glossa; labial palp flat and rounded cone, with distal sensillum. Prothorax ventrally with rows of minute cuticular proceses, such rows sparser on mesothorax and ventral metathorax. Prothoracic process absent. Hemolymph taps absent from abdominal segment IV. Abdominal segments and dorsal thoracic segments covered with dense vestiture of short erect setae; additionally, longer erect setae interspersed, sparse in most

Fig. 12. *Protanilla rong* sp. nov., paratype, gyne (CASENT0745747). **A**. Profile view. **B**. Dorsal view. Scale bars = 0.25 mm.

of abdominal segments, dense on thorax; many hairs on thorax with short cuticular spines; abdominal terminus covered in long, stout setae.

Distribution

Known only from the type locality. Putative specimens of this species collected across northern Vietnam at Ben En, Sa Pa, Vu Quang, and Xuan Son National Parks, but not included in this study, must be examined in more detail to confirm their conspecificity.

Ecology

Respective reproductive biologies of *P. wallacei* and *P. rong* sp. nov. differ in that *P. rong* is presumably monogynous, with alate gynes, whereas *P. wallacei* is polygynous, with ergatoid gynes. All *P. rong* larvae

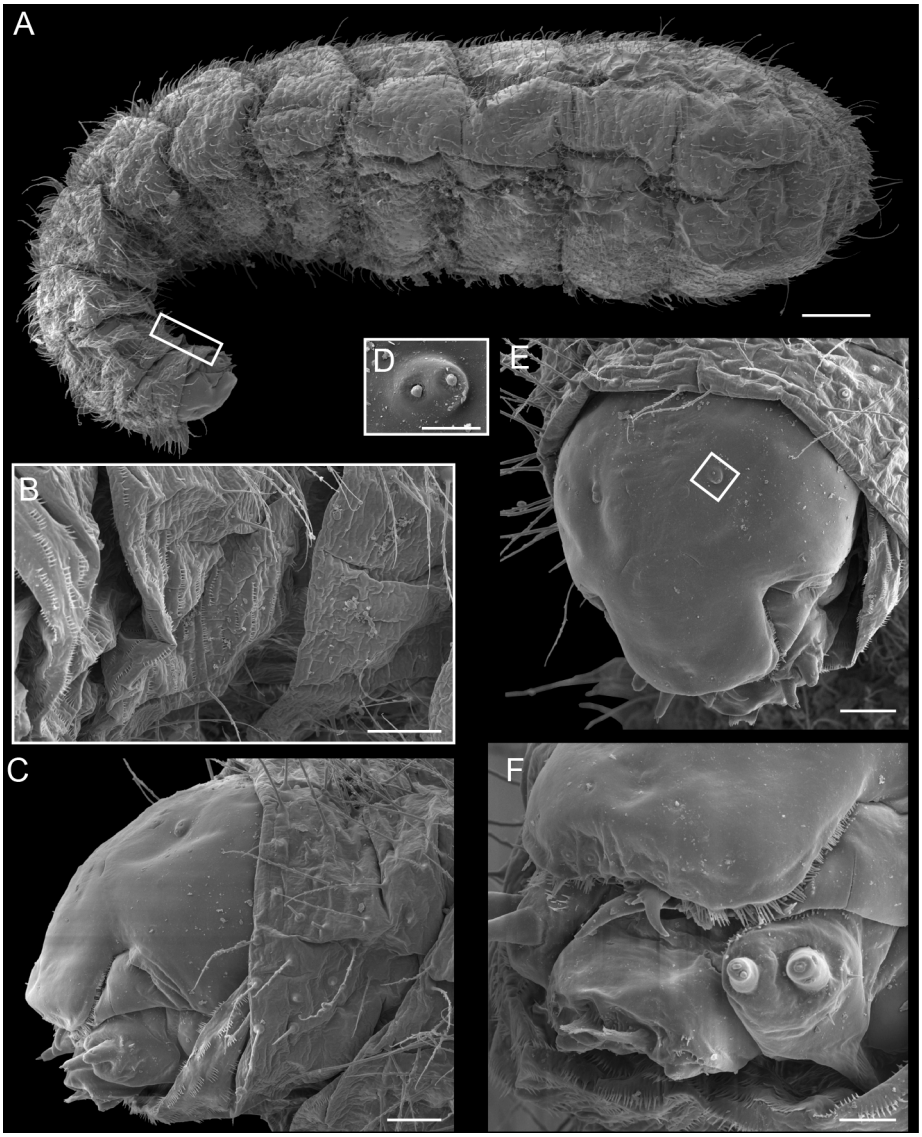

Fig. 13. *Protanilla rong* sp. nov., larva (CASENT0745741). **A**. Profile view (Fig. 13B outlined). **B**. Meso- and metathorax, ventral view. **C**. Head, profile view. **D**. Antenna. **E**. Head, anterior oblique view (Figs. 13B, D are outlined in white). **F**. Mouthparts, anterior view. Scale bars: A = 0.1 mm; B–E = 0.02 mm; F = 0.01 mm.

in the collected colony are identical in size and therefore in the same instar, suggesting synchronous brood production. Like *Leptanilla phthirigyna* sp. nov., *P. rong* was collected in a termite mound (Termitidae: Macrotermitinae), a microhabitat heretofore unobserved for the Leptanillinae, to the best of our knowledge.

Remarks

Protanilla rong sp. nov. is most similar to *Protanilla wallacei*, a species endemic to the Sundan region, differing by a more acute dorsal mandibular articulation; subpetiolar process projecting ventrad abdominal sternite III (Fig. 4A); proportional enlargement of the subpetiolar fenestra (Fig.4); and yellowish coloration. The gyne of *Protanilla rong* most closely resembles that of *Protanilla lini* among *Protanilla* in which the gyne is known (Hsu *et al.* 2017), being alate rather than the ergatoid condition observed in *P. wallacei* (Billen *et al.* 2013; Ito *et al.* 2022), but is distinguished from *P. lini* by smaller size (WL < 1.0 mm) and somewhat shorter head (CI < 85). Discovery of further gyne specimens in either species may necessitate emendation of this differential diagnosis.

Protanilla rong sp. nov. and *Protanilla wallacei* appear similar, but phylogenomic inference supports (UFBoot = 100; BPP = 1) *Protanilla rong* as sharing a more recent common ancestor with *Protanilla wardi* Bharti & Akbar, 2012 (Kerala, India), from which it differs in planarity of the anterior face of the petiolar node and smaller size (WL < 0.8 mm); and the aberrant *P. jongi* (Taiwan), from which its habitus differs far more conspicuously. The heterospecificity of *P. jongi* with relatives sampled in this study, including *P. wallacei*, is not in question; by extension, *Protanilla rong* has verity under our species concept.

Genus ***Leptanilla*** Emery, 1870

Leptanilla Emery, 1870: 196.
Scyphodon Brues, 1925: 93, fig. 1. Synonymy by Griebenow (2024: 128).
Phaulomyrma Wheeler & Wheeler, 1930: 193, figs 1–2. Synonymy by Griebenow (2021: 630).
Leptomesites Kutter, 1948: 286, figs 1–7. Synonymy by Baroni Urbani (1977: 433).
Noonilla Petersen, 1968: 582, figs 6–8. Synonymy by Griebenow (2024: 128).
Yavnella Kugler, 1987 (“1986”): 52, figs 14–22. Synonymy by Griebenow (2024: 128).

Diagnosis

Worker

1–4 medial mandibular teeth present. Ventromedial mandibular margin lacking teeth. Peg- or pencil-like chaetae absent from labrum. Dorsal mandibular articulation not visible in full-face view. Palp formula 1–2,1. Clypeus indistinct, not extending visibly between antennal toruli. Pair of medial chaetae absent from second protarsomere. Meso-metapleural suture absent; or if present, then unsculptured. Abdominal segments III–IV narrowly joined. Cuticular microsculpture present, scabriculous to areolate.

Gyne

Compound eyes repressed or present; if present then with 1–4 ommatidia. Mandible often falcate, rarely (*Leptanilla belantan* Griebenow, 2024) with distinct masticatory margin; edentate, or with 1–2 subapical teeth. Wings and alar sclerites absent. Abdominal segment III not petiolate.

Male

Palp formula 1–2,1. Ocelli present or absent; if present, then almost always set on tubercle. Notauli absent. Pterostigma absent. Hindwing 1A absent. Volsellae present or absent; if present, then parossiculus and lateropenite insensibly fused. Cupula present or absent; if present, then annular. Penial sclerites medially fused, rarely (*Leptanilla astylina* Petersen, 1968; *Leptanilla* TH03) articulated.

Key to *Leptanilla* workers of the Eastern Palaearctic and Indo-Malaya

Condensed from Griebenow (2024: 148–149, 152–154), with the addition of taxa described since that publication (Qian *et al.* 2024; Zhong 2024).

1. Clypeus with median process (Fig. 3C) 2
– Clypeus without median process (Fig. 3A) 16

2. Clypeal process entire; length of abdominal postsclerites IV < combined length of abdominal postsclerites V–VIII 3
– Clypeal process emarginate to bilobed; length of abdominal postsclerites IV ≥ combined length of abdominal postsclerites V–VIII 5

3. Posteriorly recurved subpetiolar process absent; PPI = 80–86 ..... ***Leptanilla buddhista*** Baroni Urbani, 1977 (NEPAL)
– Posteriorly recurved subpetiolar process present; PPI = 122–138 4

4. CI = 72–74, SI = 49–56; outline of antennal torulus subcircular (Zhong 2024: fig. 3c) ..... ***Leptanilla macauensis*** Leong *et al.*, 2018 (CHINA: Macau)
– CI = 67–70, SI = 63–66; outline of antennal torulus oblong, with protruding anteromedial angle (Zhong 2024: fig. 3b) ..... ***Leptanilla sichuanensis*** Zhong, 2024 (CHINA: Sichuan)

5. Anterior margin of dorsal petiolar node emarginate in dorsal view (Leong *et al*. 2018: fig. 13e–f) 6
– Anterior margin of dorsal petiolar node entire in dorsal view (Leong *et al*. 2018: fig. 13a, d) 7

6. Dorsal petiolar node almost twice as long as wide in dorsal view ..... ***Leptanilla hypodracos*** Wong & Guénard, 2016 (SINGAPORE)
– Length and width of dorsal petiolar node subequal in dorsal view; postpetiolar node distinctly wider than long in dorsal view ..... ***Leptanilla clypeata*** Yamane & Ito, 2001 (INDONESIA: Java)

7. Length of metasomal setae bimodal 8
– Length of metasomal setae unimodal 11

8. Mandible with four teeth, with most proximal tooth truncate (Saroj *et al*. 2022: fig. 1e); ventromedian lamella of abdominal sternite II denticulate ..... ***Leptanilla ujjalai*** Saroj *et al.*, 2022 (INDIA: West Bengal)
– Mandible with three teeth, with most proximal tooth not truncate; ventromedian lamella of abdominal sternite II not denticulate 9

9. Longitudinal subpetiolar lamella absent ..... ***Leptanilla dehongensis*** Qian *et al.*, 2024 (CHINA: Yunnan)
– Longitudinal subpetiolar lamella present 10

10. Lateral pronotal margins weakly convex in dorsal view; PPTI = 74–76 ..... ***Leptanilla lamellata*** Bharti & Kumar, 2012 (INDIA: Himachal Pradesh)
– Lateral pronotal margins strongly convex in dorsal view; PPTI = 85–86 ..... ***Leptanilla escheri*** (Kutter, 1948) (INDIA: Tamil Nadu)

11. PI > 85 12
– PI ≤ 85 15

12. Mandible with three teeth, most proximal tooth acute ..... ***Leptanilla kunmingensis*** Xu & Zhang, 2002 (CHINA: Yunnan)
– Mandible with four teeth, most proximal tooth blunt 13

13. Meso-metapleural suture present laterally; PPI≤87 ..... ***Leptanilla sapa*** Yamada sp. nov. (VIETNAM: Lao Cai)
– Meso-metapleural suture absent laterally; PPI>87 14

14. Proximal mandibular tooth recurved, apex expanded ..... ***Leptanilla belantan*** Griebenow, 2024 (MALAYSIA: Selangor)
– Proximal mandibular tooth sublinear, apex not expanded ..... ***Leptanilla belantanoides*** sp. nov. (VIETNAM: Ninh Binh)

15. Subpetiolar process present, angular; torular rim without areolate sculpture (Griebenow 2024: fig. 27a) ..... ***Leptanilla havilandi*** Forel, 1901 (SINGAPORE; MALAYSIA: Sabah)
– Subpetiolar process absent; torular rim with medial and anterior areolate sculpture (Griebenow 2024: fig. 27b)..... ***Leptanilla thai*** Baroni Urbani, 1977 (THAILAND: Khao Chong)

16. Mandible with two teeth 17
– Mandible with 3–4 teeth 18

17. Anterior margin of cranium with anterolateral clypeal projections; ventral vertices of abdominal sternites II–III projecting a subequal distance ventrad craniocaudal axis ..... ***Leptanilla kebunraya*** Yamane & Ito, 2001 (INDONESIA: Java)
– Anterior margin of cranium entire; ventral vertex of abdominal sternite II distinctly lower on dorsoventral axis compared to ventral vertex of abdominal sternite III ..... ***Leptanilla butteli*** Forel, 1913 (MALAYSIA: Selangor)

18. Meso-metapleural groove present, impressed on dorsum of mesosoma ..... ***Leptanilla hunanensis*** Tang *et al*., 1992 (CHINA: Hunan)
– Meso-metapleural groove absent from dorsum of mesosoma, sometimes impressed on sides 19

19. Clypeus with median emargination 20
– Anterior clypeal margin entire, sublinear to convex 23

20. Abdominal tergite IV not narrowed anteriorly in dorsal view (Griebenow 2024: fig. 36b); clypeal margin protruding well anterad antennal toruli ..... ***Leptanilla oceanica*** Baroni Urbani, 1977 (JAPAN: Ogasawara Islands)
– Abdominal tergite IV narrowed anteriorly in dorsal view (Griebenow 2024: fig. 36a); clypeal margin not protruding well anterad antennal toruli 21

21. Abdominal tergite II trapezoidal in dorsal view, narrowing posteriorly; abdominal sternite III nearly planar ..... ***Leptanilla qinlingensis*** Qian *et al.*, 2024 (CHINA: Shaanxi)
– Abdominal tergite II rectangular in dorsal view, not narrowing posteriorly; abdominal sternite II convex 22

22. Mandibular teeth equidistant (Zhong 2024: fig. 13a) ..... ***Leptanilla taiwanensis*** Ogata *et al.*, 1995 (TAIWAN)
– Proximal mandibular tooth slightly removed from remaining teeth (Zhong 2024: fig. 13b) ..... ***Leptanilla beijingensis*** Qian *et al.*, 2024 (CHINA: Beijing)

23. Mandible with four teeth (subapical tooth sometimes difficult to distinguish) 24
– Mandible with three teeth 25

24. Most proximal mandibular tooth large and distinct; abdominal tergite IV distinctly narrowed anteriorly in dorsal view .....***Leptanilla tanakai*** Baroni Urbani, 1977 (JAPAN: Yakushima)
– Most proximal mandibular tooth small and indistinct; abdominal tergite IV not distinctly narrowed anteriorly in dorsal view .....***Leptanilla japonica*** Baroni Urbani, 1977 (JAPAN: Honshu)

25. Petiole distinctly wider than long .....***Leptanilla yunnanensis*** Xu, 2002 (CHINA: Yunnan)
– Petiole not distinctly wider than long 26

26. Anterior margin of clypeus convex in full-face view 27
– Anterior margin of clypeus linear in full-face view 28

27. Mesothorax anteriorly constricted in dorsal view ....***Leptanilla besucheti*** Baroni Urbani, 1977 (SRI LANKA)
– Mesothorax not anteriorly constricted in dorsal view ....***Leptanilla morimotoi*** Yasumatsu, 1960 (JAPAN: Kyushu)

28. Pedicel length and width subequal .... ***Leptanilla okinawensis*** Terayama, 2013 (JAPAN: Okinawa)
– Pedicel distinctly longer than wide 29

29. Meso-metapleural suture absent; subpetiolar process absent posteriorly, abdominal sternite II linear in profile view .....***Leptanilla kubotai*** Baroni Urbani, 1977 (JAPAN: Shikoku)
– Meso-metapleural suture present on side of mesosoma, absent from dorsum; abdominal sternite II convex in profile view .....***Leptanilla phthirigyna*** sp. nov. (VIETNAM: Ninh Binh)

Leptanilla belantanoides sp. nov.
urn:lsid:zoobank.org:act:8BBE61F2-2D95-41EB-B7A0-857E40222303
Figs 14–15

Surface mesh of worker: https://sketchfab.com/3d-models/casent0745758-leptanilla-belantanoides-worker-27a618e409664d6e874cbd978d73f163

Diagnosis

Worker

Mandible with four teeth, basal tooth truncate; short relative to head. Scape short relative to head. Flagellum submoniliform. Clypeal process present, apex emarginate. Length of subapical tapering seta <½ ML. Maxillary palp 1-merous. PrW > MW. Pronotal and mesonotal heights of dorsa subequal. Meso-metapleural suture absent. Anterior margin of abdominal segment II linear in dorsal view. Subpetiolar process present, not lamellate. PTL < PPL. Abdominal sternites II–III projecting comparably ventrad craniocaudal axis. PPW <½ TW4. Length of abdominal postsclerites IV greater than combined length of abdominal postsclerites V–VIII.

Male

Mandibles inarticulate. Clypeus distinct, extending between toruli; antennal sockets not placed on anterior cranial shelf. LF2 and ML > SL. Ocelli present, situated on tubercle; anteromedian ocellus directly dorsad compound eyes in profile view. Distal transverse carina absent from procoxa; protrochanter sphenoid; profemur arcuate, arcuate medial carina and apicoventral hook absent; ventromedian carina and cuticular comb absent from protibia. Pronotum and mesoscutum not anteroposteriorly prolonged. Mesoscutellum without posterior process. Forewing M+Cu absent.

Metapleuron distinct from metapectal-propodeal complex. Propodeal declivity concave in profile view. Petiole without distinct dorsal node. Abdominal tergite VIII broader than long in posterodorsal view. Mulceators absent. Gonopodites inarticulate, with ventral suture; gonocoxites without dorsomedian fusion; gonostyli present, ventral margins entire and not dorsad ventral gonocoxital margins. Volsellae present, medially separate; apex furcated. Penial sclerites dorsoventrally compressed, medially fused; phallotreme dorso-apical, without setal vestiture.

Etymology

The specific epithet means 'like *belantan*', referring to *Leptanilla belantan*, a closely related species. The gender of the specific epithet is neuter.

Type material

Holotype

VIETNAM – **Ninh Binh** • worker; Cuc Phuong National Park, 150 m NW of central parking lot; 20.3492° N, 105.5970° E; 392 m a.s.l.; 8 Aug. 2022; A. Richter leg.; clay soil by rotten log, ~2 cm deep; ARVI0042 ; IEBR, CSUENT6000061.

Paratypes

VIETNAM – **Ninh Binh** • 4 workers; same data as for holotype; IEBR, CASENT0842867, CASENT0842878, CASENT0842879, CASENT0842881.

Other material examined

VIETNAM – **Ninh Binh** • 2 workers; same data as for preceding; IEBR, CASENT0842880, CASENT0842882 • 1 ♂; Cuc Phuong National Park, headquarters; 20.25014° N, 105.70469° E±6 m; 190 m a.s.l.; 7 Aug. 2022; P.S. Ward leg.; PSW18689-01; UCDC, CASENT0842868 • 1 ♂; same data as for preceding; IEBR, CASENT0842869 • 1 ♂; Cuc Phuong National Park, headquarters; 20.24790° N, 105.70871° E±4 m; 160 m a.s.l.; 7 Aug. 2022; P.S. Ward leg.; PSW18688-01; P.S. Ward personal collection, CASENT0883690.

Measurements and indices

Holotype

HW = 0.31 mm; HL = 0.41 mm; SL = 0.25 mm; ML = 0.17 mm; WL = 0.52; PrW = 0.21 mm; MW = 0.15 mm; PTL = 0.12 mm; PTH = 0.11 mm; PTW = 0.10 mm; PPL = 0.10 mm; PPW = 0.10 mm; PPH = 0.14 mm; TW4 = 0.30 mm; CI = 76; SI = 81; MI = 55; PI = 83; PPI = 100; TI1 = 33.

Workers

HW = 0.31–0.32 mm; HL = 0.40–0.41 mm; SL = 0.24–0.26 mm; ML = 0.16–0.17 mm; WL = 0.51–0.53 mm; PrW = 0.18–0.20 mm; MW = 0.13–0.15 mm; PTL = 0.11–0.13 mm; PTH = 0.11–0.12 mm; PTW = 0.08–0.10 mm; PPL = 0.09–0.10 mm; PPW = 0.09–0.10 mm; PPH = 0.14 (n = 4); TW4 = 0.28–0.30 mm; CI = 75–79; SI = 75–85; MI = 51–55; PI = 65–93; PPI = 91–106; TI1 = 32–36.

Male

HW = 0.36 mm; HL = 0.23 mm; SL = 0.11 mm; LF2 = 0.15 mm; MaL = 0.04 mm; ML = 0.06 mm; EW 0.16 mm; EL = 0.13 mm; WL = 0.65 mm; MSW = 0.32 mm; MSL = 0.33 mm; PTL = 0.08 mm; PTH = 0.16 mm; PTW = 0.17 mm; CI = 158; SI = 30; MI = 17; OI = 82; REL = 56; MSI = 98; PI = 206.

Description

Worker

Lateral margins of cranium moderately convex. Occipital carina distinct. Clypeal process present, delimited from cranium by lateral carinae, with posteromedian delimitation from cranium by Λ-shaped

signum, projecting well anterior of labrum in full-face view; apex robust, broad in outline, linear, bordered by laminae. Mandible short relative to head; four teeth present; basal tooth large, blunt, not enlarged apically nor distally recurved. Large, tapering basal seta absent from mandible; subapical tapering seta present, only slightly longer than surrounding setae, <½ ML. Maxillary palp 1-merous. Pedicel length subequal to that of basal flagellomere. Flagellum submoniliform; antennomere 3 subequal in length to distal antennomeres; apical flagellomere >2× as long as subapical flagellomere. In dorsal view, pronotal margins strongly convex, pronotal width distinctly greater than mesonotal width (PrW = 0.18–0.21 mm; MW = 0.13–0.15 mm). Pronotal dorsum slightly convex, elevation equal to that of dorsal mesonotal vertex. Lateral margins of mesonotum and metapectal-propodeal complex subparallel in dorsal view; mesonotum not constricted anteriorly. Meso-metapleural suture absent; fusion of mesonotum with propodeum marked by shallow excavation. Bulla extending anterad propodeal spiracle. Propodeum angular in profile view; propodeal declivity slanted; posterolateral corners rounded. Tarsomeres longer than broad. Meso- and metatibial spur formula 2b,2(1b,1p). Anterior margin of petiole linear in dorsal view. Abdominal segment II longer than wide, with distinct dorsal node; margins parallel in dorsal view; subpetiolar process present, not lamellate, anterior face concave in profile view. Abdominal segment III longer than wide in dorsal view. Breadth of abdominal segment III less than half the breadth of abdominal segment IV in dorsal view. Anteroposterior length of abdominal tergite IV greater than that of V–VIII combined. Mesopectus and ventral surface of petiolar sternite without reticulate sculpture. Coloration castaneous.

Male

Cranial outline subspherical (CI = 158). Occiput entire. Frons not produced into anterior shelf. Mandible fused to gena; broader than long. Mandalus large, covering entire ectal mandibular surface.

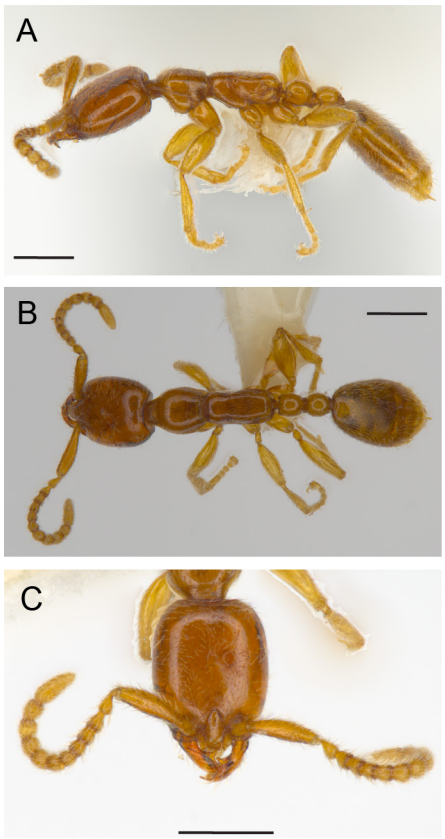

Fig. 14. *Leptanilla belantanoides* sp. nov., holotype, worker (CSUENT6000061). **A**. Profile view. **B**. Dorsal view. **C**. Full-face view. Scale bars = 0.25 mm.

Maxillary palp 2-merous, palpomeres indistinct. Clypeus extending posteriorly between antennal toruli, discernible in full-face view. Anterior tentorial pits situated anterad antennal toruli. Compound eyes wider than long in profile view (OI = 82), large (REL = 56), outline subcircular, all margins entire. Anteromedian ocellus and compound eyes both intersecting line drawn perpendicular to anteroposterior axis of cranium. Scape subcircular in cross-section, longer than wide, SL < EL; pedicel short, vasiform, length 0.5× SL; antennomere 3 long, cylindrical, length greater than that of scape (SL = 0.11 mm; LF2 = 0.15 mm); flagellum filiform, extending posterior to mesoscutum if folded flat over mesosoma. Pronotum and mesoscutum not anteroposteriorly prolonged. In profile view anterodorsal pronotal face diagonal to craniocaudal axis at ~45° angle. Mesoscutal dorsum convex, projecting anteriorly dorsad pronotum; mesoscutum longer than broad. Antero-admedian signum present. Notauli absent. Parapsidal signa present, impressed. Mesoscutellum as tall as long, dorsum higher than that of mesoscutum, posterodorsal mesoscutellar face convex, not posteriorly produced or recurved. Oblique mesopleural sulcus present, not intersecting metapectal-propodeal complex. Metapleuron distinct, juncture between upper and lower metapleuron narrow. Metapleural gland absent. Propodeum concave in profile view, with outline sinuate. Coxal lengths subequal, with procoxal length greatest. Procoxa without distal transverse carina. Protrochanters sphenoid in outline, distally truncate. Profemur slightly curved, with proximal dorsoventral margins converging in lateral view, not anteroposteriorly compressed; acute distal flange on ventral surface absent; arcuate medial carina absent. Protibia slightly shorter than profemur; not dorsoventrally compressed, without ventromedian carina; protibial comb absent; probasitarsal seta smaller than calcar. Spur formula 2b,2b. C and Sc+R+Rs fused, tubular; *2s-rs*+R+4-6, Rsf1, Mf1, and M+Cu nebulous; all other venation absent. Costal infuscation absent. Abdominal segment II anteroposteriorly compressed, broader than long in dorsal view (PI = 206), excluding presclerites; dorsal node absent; without median dorsal excavation. Abdominal sternite II without process, convex in profile view. Presclerites of abdominal segments III–VIII inconspicuous. Abdominal segments III–VII without tergosternal fusion. Tergosternal fusion of abdominal segments VIII–IX unknown. Abdominal tergites III–VII anteroposteriorly compressed, lateral margins subparallel or converging; breadth of abdominal tergite VIII subequal to that of abdominal tergite VII in posterodorsal view. Abdominal sternites VIII–IX not visible without dissection. Mulceators absent. Gonopodite inarticulate. Gonocoxites without complete dorsomedian and ventromedian fusion; gonocoxital lamina absent. Gonostylus present, recurved medially, with expansive dorsal laminae; apex entire. Volsella present, transected by articulatory sulcus; bifid, with dorsal process sharply curving laterally, ventral process moderately curving laterally, apex extending distad that of dorsal process. Penial sclerites dorsoventrally compressed, not basally recurved, dorso- and ventromedian carinae absent, lateral margins laminate. Penial apex with deep median incision, phallotreme at proximal extremity of incision. Phallotreme dorsal, apical, not recessed, not surrounded by vestiture of setae. Most sclerites with vestiture of subdecumbent setae; elongated on posterior margins of abdominal tergites VII–VIII; ventral face of volsella distad articulatory sulcus with long, suberect setae; gonostylus with decumbent setae, longer than on soma; genitalia otherwise bare. Cuticle bearing piligerous punctae; sculpture otherwise absent.

Distribution

Known only from Cuc Phuong National Park.

Ecology

Little is definitively known, or can be speculated, regarding the ecology of *Leptanilla belantanoides* sp. nov. The habitation of this species in soil is unremarkable for *Leptanilla*.

Remarks

Leptanilla belantanoides sp. nov. appears most similar to *L. belantan* from peninsular Malaysia and *Leptanilla sapa* sp. nov., with the shape of the proximal mandibular tooth being intermediate in

L. belantanoides between these two species, and its length proportionally shorter than in *L. belantan*. Emargination of the clypeal process is also less pronounced in the worker caste of *L. belantanoides* than in either of these relatives. Further sampling of worker members of the *Leptanilla thai* species-group across mainland southeast Asia, and collection of the corresponding males, will clarify the boundaries between these species.

In the male-based key to the *Leptanilla thai* species-group of Griebenow (2024: 162), *Leptanilla belantanoides* sp. nov. keys out to the second lug of couplet 9. It is distinguished from *Leptanilla* zhg-th05 in that the ventral gonostylar margin is entire, without any projecting angle; and that the ventral

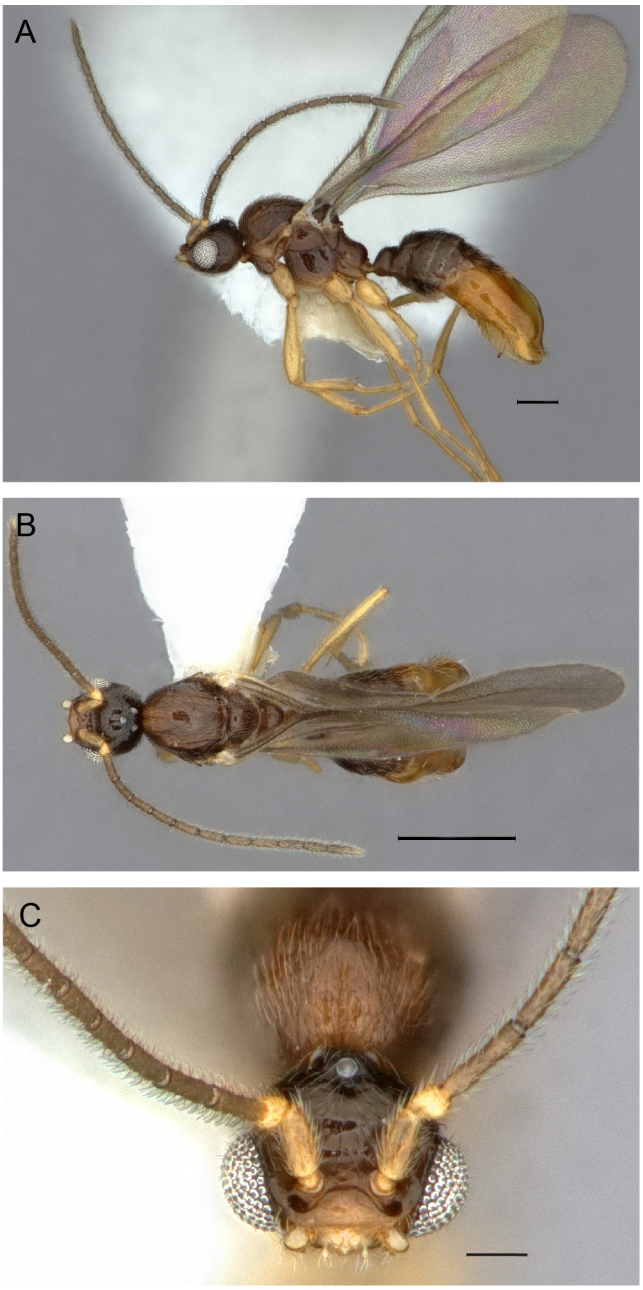

Fig. 15. *Leptanilla belantanoides* sp. nov., male (CASENT0842869). **A**. Profile view. **B**. Dorsal view. **C**. Full-face view. Scale bars: A = 0.2 mm; B = 0.5 mm; C = 0.01 mm.

gonopodital suture is not coincident with an abrupt ledge. As in *Leptanilla* zhg-th05 and several other male morphospecies within the *Leptanilla thai* species-group, the dorsoventral margins of the male profemur in *Leptanilla belantanoides* converge proximally, giving the profemur an arcuate outline in profile (Griebenow 2024: fig. 42A). We predict that the male profemur of *Leptanilla belantanoides* serves a grasping function in copula.

Leptanilla belantanoides sp. nov. is here confirmed to belong to the *Leptanilla thai* species-group by phylogenomic inference. Beyond *L. belantan* and *Leptanilla sapa* sp. nov., among the putative members of the *Leptanilla thai* species-group for which the worker caste is known, *L. belantanoides* appears is most closely similar to *Leptanilla ujjalai* Saroj *et al.*, 2022 and the undescribed *Leptanilla* zhg-th02. Males are unknown for these relatives of *L. belantanoides*, and none have yet been sequenced. All are united in possessing a truncate proximal tooth on the worker mandible, ventrad the masticatory margin.

The *Leptanilla thai* species-group, equivalent to the former genus *Yavnella*, was originally described from male specimens (Kugler 1987), with the worker caste being heretofore definitively identified only for *Leptanilla laventa* (Griebenow *et al.*, 2022). The male is unknown in both these species, meaning that *L. belantanoides* is the first member of the *Leptanilla thai* species-group for which the worker and male are associated (in this case by UCEs). The male morphospecies that most closely resemble those of *L. belantanoides* sp. nov. are all undescribed.

Leptanilla sapa Yamada sp. nov.
urn:lsid:zoobank.org:act:E28E31C4-959D-43D4-BA12-24E43BF259AA
Figs 16–17, 18Aii

Surface mesh of worker: https://sketchfab.com/3d-models/casent0745756-leptanilla-sapa-worker-ab5316ce932d4337a96edd278ec52e23
Surface mesh of gyne: https://sketchfab.com/3d-models/casent0745762-leptanilla-sapa-queen-28da0ae5cc904a47965eeda0cef2d1e1

Diagnosis

Worker

As for *Leptanilla belantanoides* sp. nov., but with the differences stipulated under Description.

Gyne

Mandible falcate, without distinct basal and masticatory margins, edentate, with two weak blunt denticles. Anterior clypeal margin slightly convex, with median elevation. Compound eye present, with four ommatidia. Meso-metapleural suture laterally present. Abdominal segment II longer than broad, without distinct dorsal node; subpetiolar process absent; rectangular, not constricted anteriorly along anteroposterior or lateromedian axes.

Etymology

From Sa Pa, the type locality of this species. The specific epithet is a noun in apposition and therefore invariant.

Type material

Holotype

VIETNAM – **Lao Cai** • worker; Hoang Lien National Park, Sa Pa, Mt. Phan Xi Pang, Cong Troi; 1800–1900 m a.s.l.; 8 Oct. 2006; K. Eguchi leg.; Eg08x06-12; IEBR, CASENT0745756.

Paratypes

VIETNAM – **Lao Cai** • 1 gyne; same data as for holotype; IEBR, CASENT0745762 • 12 workers; same data as for holotype; IEBR, CSUENT6000020 to CSUENT6000031.

Other material examined

VIETNAM – **Lao Cai** • 2 workers; Hoang Lien National Park, Sa Pa, Mt Phan Xi Pang, Cong Troi; 2000–2200 m a.s.l.; 28 Apr. 2002; K. Eguchi leg.; Eg02-VN-155; IEBR, CSUENT6000032, CSUENT6000033 • 3 workers; same locality as for preceding; 28 Apr. 2002; K. Eguchi leg.; Eg02-VN-151; Katsuyuki Eguchi personal collection, CSUENT6000041 to CSUENT6000043 • 2 workers; Hoang Lien National Park, Sa Pa, Mt Phan Xi Pang; 22.35121° N, 103.77642° E; 2000 m a.s.l.; 20 Sep. 2017; K. Eguchi leg.; Eg24ix17-378; IEBR, CSUENT6000034, CSUENT6000035 • 5 workers; same locality as for preceding; 22.34609° N, 103.77459° E; 2008 m a.s.l.; 27 Sep. 2017; K. Eguchi leg.; Eg27ix17-451; IEBR, CSUENT6000036 to CSUENT6000040 • 3 workers; same locality as for preceding; 22.34600° N, 103.77469° E; 2006 m a.s.l.; 27 Sep. 2017; K. Eguchi leg.; Eg27ix17-447; Katsuyuki Eguchi personal collection, CSUENT6000044 to CSUENT6000046.

Measurements and indices

Holotype

HW = 0.36 mm; HL = 0.49 mm; SL = 0.27 mm; ML = 0.25 mm; WL = 0.61 mm; PrW = 0.24 mm; MW = 0.18 mm; PTL = 0.18; PTH = 0.13 mm; PTW = 0.11 mm; PPL = 0.13 mm; PPW = 0.11 mm; PPH = 0.17 mm; TW4 = 0.35 mm; CI = 74; SI = 74; MI = 68; PI = 59; PPI = 83; TI1 = 32.

Worker paratypes

HW = 0.37–0.39 mm; HL = 0.48–0.54 mm; SL = 0.26–0.31 mm; ML= 0.22 –0.26 mm; WL = 0.62–0.71 mm; PrW = 0.25–0.28 mm; MW = 0.18–0.20 mm; PTL = 0.18–0.22 mm; PTH = 0.13–0.15 mm; PTW = 0.11–0.12 mm; PPL = 0.14–0.16 mm; PPW = 0.12–0.13 mm; PPH = 0.19–0.21 mm; TW4 = 0.35–0.40 mm; CI = 74–77; SI = 71–77; MI = 60–65; PI = 55–58; PPI = 76–87; TI1 = 30–35.

Paratype gyne

HW = 0.56 mm; HL = 0.65 mm; ML = 0.41 mm; WL = 1.11 mm; PrW = 0.38 mm; MW = 0.38 mm; PTL = 0.63 mm; PTH = 0.32 mm; PTW = 0.39 mm; CI = 87; SI = 65; MI = 72; PI = 61.

Description

Worker

As in *Leptanilla belantanoides* sp. nov., but clypeal process posteromedially not clearly delimited from cranium; apex strongly bilobed with distinctly concave anterior margin (Fig. 18Aii). Proximal mandibular tooth about twice as long as wide, distally slightly recurved. Pronotal dorsum moderately convex, slightly elevated above dorsal mesonotal vertex. Meso-metapleural suture indistinct, faintly furrowed. Bulla reaching propodeal spiracle but not extending anterad. Propodeum rather rounded in profile view; propodeal declivity slanted; posterolateral corners rounded. Tibial spur formula 2b,2(1b,1p). Margins of abdominal segment II subparallel, slightly convex around node in dorsal view. Breadth of abdominal segment III less than half the breadth of abdominal segment IV in dorsal view (TI1 = 30–35). Mesopectus and ventral surface of petiolar sternite with reticulate sculpture. Coloration castaneous.

Gyne

Labrum deeply emarginate. Cranium in full-face view subrectangular, widest at level of midpoint of genae below eyes; occipital margin linear. Clypeal process absent. Mesonotum laterally delimited from mesopleuron by furrow. In dorsal view, breadth of mesonotum less than that of pronotum or metanotal-propodeal complex. Propodeum with distinct declivity. Abdominal segment II dorsoventrally compressed, subcylindrical, longer than wide, without distinct dorsal node; margins subparallel in dorsal view, weakly converging posteriorly; subpetiolar process absent. In dorsal view, abdominal segment III not conspicuously narrower than abdominal segment IV; axial relative to posterad abdominal segments.

Abdominal postsclerites III shorter than postsclerites IV–VII; the latter subequal in length. Vestiture consists of short subdecumbent to suberect setae, longer and more abundant on gaster than on remainder of soma. Coloration pallid.

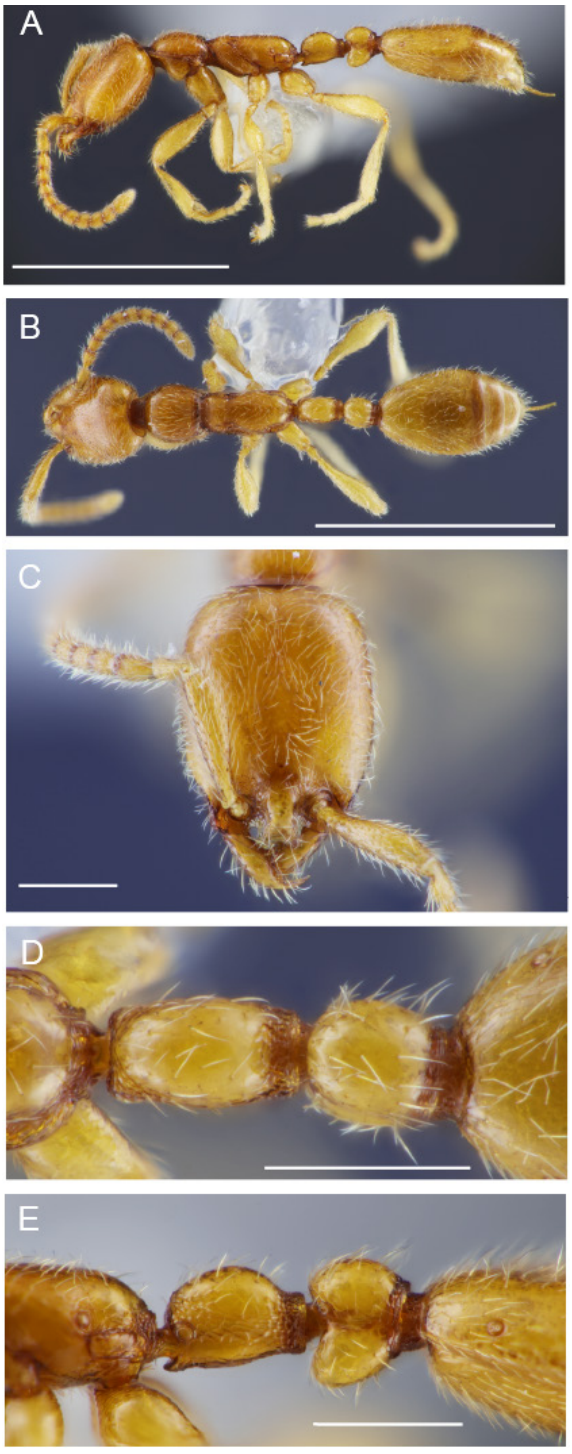

Fig. 16. *Leptanilla sapa* Yamada sp. nov., holotype, worker (CASENT0745756). **A**. Full-face view. **B**. Profile view. **C**. Dorsal view. **D**. Abdominal segments II–III, profile view. **E**. Abdominal segments II–III, dorsal view. Scale bars: A–B = 1 mm; C = 0.2 mm.

Distribution

Known only from the type locality.

Ecology

Leptanilla sapa sp. nov. is relatively common in the vicinity of Sa Pa, corresponding to *Leptanilla* sp. eg-1 reported by Eguchi *et al.* (2014: 22). The colonies were found under moss layers in a cloud forest (K. Eguchi pers. com.). One colony (Eg27ix17-447) contained a paralyzed mecistocephalid centipede (Chilopoda: Geophilomorpha) fed upon by larvae. The upper limit of the elevational range of *L. sapa* sp. nov. (2200 m) surpasses that reported for any other *Leptanilla* – only its close relative *L. ujjalai* and

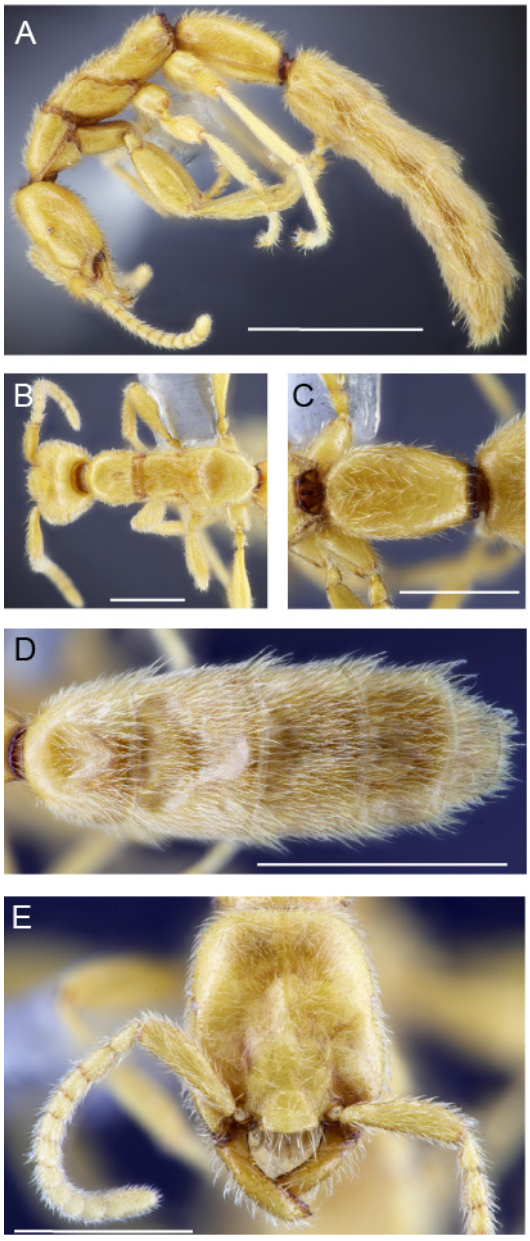

Fig. 17. *Leptanilla sapa* Yamada sp. nov., paratype, gyne (CASENT0745762). **A**. Full-face view. **B**. Profile view. **C**. Mesosoma and head, dorsal view. **D**. Abdominal segment II, dorsal view. **E**. Abdominal segments III–VII, dorsal view. Scale bars: A, D = 1 mm; B–C, E = 0.5 mm.

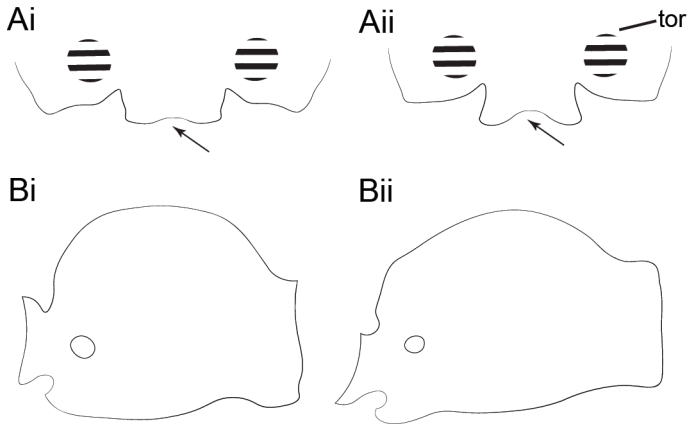

Fig. 18. Diagrammatic comparison of *Leptanilla belantanoides* sp. nov. (i) and *Leptanilla sapa* Yamada sp. nov. (ii). **A**. Anterior outline of cranium, with anterior margin of clypeal process indicated by arrow. **B**. Abdominal segment II, profile view. Abbreviation: tor = torulus.

an undescribed male morphospecies of the *Leptanilla revelierii* species-group (*Leptanilla* zhg-my09) approach this, being collected at 2014 m and 1900 m, respectively (Saroj *et al.* 2022: 6; AntWeb 2024).

Remarks

Leptanilla sapa sp. nov. is doubtlessly a close relative of *Leptanilla belantanoides* sp. nov. and *Leptanilla belantan*, and therefore belongs to the *Leptanilla thai* species-group. The worker caste differs from both these species in that the apex of the truncate proximal tooth of the mandible is not at all expanded, nor is this tooth recurved distally; and in that the meso-metapleural suture is distinctly present laterally. Abdominal segment III is proportionally longer in worker *L. sapa* sp. nov. than in either of these species (PPI = 73–88), while abdominal segment II is also proportionally longer in *L. sapa* than in *L. belantanoides* (Fig. 18B).

While the phenotype of the worker caste differs little among *L. sapa* sp. nov. and its close relatives, the gyne of this species diverges conspicuously from that of *L. belantan* in the presence of compound eyes, with more ommatidia than ever before described in *Leptanilla*; falcate mandible, without distinct masticatory margin; presence of distinctly impressed meso-metapleural suture; and subrectangular abdominal segment II, lacking the anterior constriction observed in *L. belantan* along the dorsoventral and lateromedian axes, longer than any of the posterad abdominal segments. This striking differentiation in the gyne corroborates the allospecificity of *L. sapa* with *L. belantan*.

It remains possible that the phenotypic differences among these three allopatric species in fact represent regional variation in a single geographically widespread species. This could only be falsified by the discovery of two or more of these species in sympatry, while maintaining morphometric distinctness. For the time being, we are confident that *Leptanilla sapa* sp. nov., *Leptanilla belantanoides* sp. nov. and *L. belantan* represent distinct species, since the differentiation in the worker caste among these putative species is qualitatively equivalent to that observed between *Leptanilla charonea* and *Leptanilla zaballosi* Barandica *et al.*, 1994, which occur in sympatry and are indubitably allospecific (López *et al.* 1994; Griebenow 2024). Description of the unknown male of *L. sapa* will be invaluable for assessing its distinctness from *L. belantanoides*.

Leptanilla phthirigyna sp. nov.
urn:lsid:zoobank.org:act:DF5632D4-B877-481D-B991-81FC1D064A51
Figs 19–20

Diagnosis

Worker

Mandible with three teeth, short relative to head. Scape short relative to head. Flagellum submoniliform. Clypeal process absent; clypeal margin linear, entire. Length of subapical tapering seta ~ ½ ML. PrW ≈ MW. Pronotal and mesonotal heights of dorsa subequal. Meso-metapleural suture absent from dorsum. Anterior margin of abdominal segment II linear in dorsal view. Subpetiolar process present, not lamellate. PTL ≈ PPL. Abdominal sternites II–III projecting comparably ventrad craniocaudal axis. PPW ~ ½ TW4. Length of abdominal postsclerites IV less than combined length of abdominal postsclerites V–VIII.

Gyne

Mandible falcate, without distinct basal and masticatory margins, subapical tooth present; strongly bowed inward. Anterior clypeal margin slightly convex, without median elevation. Compound eyes absent. Meso-metapleural suture absent. Abdominal segment II as broad as long, with distinct dorsal node; subpetiolar process absent; quadrate, not constricted anteriorly along anteroposterior or lateromedian axes.

Etymology

From the Greek '*phthirus*', meaning 'louse', and '*gyna*', that is, 'gyne'. This refers to the minute size and dorsoventral compression of the gyne, which along with elongate vestiture on the metasoma grants an ectoparasitic gestalt. Gender of specific epithet is feminine.

Type material

Holotype

VIETNAM – **Ninh Binh** • worker; Cuc Phuong National Park; 20.3496° N, 105.5957° E; 400 m a.s.l.; 8 Aug. 2022; M.G. Branstetter leg.; #4349; in macrotermitine mound; IEBR, CSUENT6000054.

Paratypes

VIETNAM – **Ninh Binh** • 1 gyne; same data as for holotype; IEBR, CASENT0842890 • 2 workers; same data as for holotype; IEBR, CASENT0842891, CASENT0842892.

Other material examined

VIETNAM – **Ninh Binh** • 1 gyne; same data as for holotype; IEBR, CASENT0842889.

Measurements and indices

Holotype

HW = 0.20 mm; HL = 0.26 mm; SL = 0.13 mm; ML = 0.11 mm; WL = 0.33 mm; PrW = 0.13 mm; MW = 0.11 mm; PTL = 0.08 mm; PTH = 0.09 mm; PTW = 0.07 mm; PPL = 0.07 mm; PPW = 0.09 mm; PPH = 0.10 mm; TW4 = 0.20 mm; CI = 76; SI = 63; MI = 53; PI = 88; PPI = 125; TI1 = 43.

Paratype workers

HW = 0.21–0.22 mm; HL = 0.26–0.27 mm; SL = 0.13 mm; ML = 0.10–0.11 mm; WL = 0.34–0.35 mm; PrW = 0.13–0.14 mm; MW = 0.12 mm; PTL = 0.09 mm; PTH = 0.09–0.10 mm; PTW = 0.08–0.09 mm; PPL = 0.08 mm; PPW = 0.09–0.10 mm; PPH = 0.11–0.12 mm; TW4 = 0.20–0.21 mm; CI = 78–81; SI = 60–61; MI = 47–52; PI = 85–99; PPI = 113–123; TI1 = 46–48.

Paratype gyne

HW = 0.28 mm; HL = 0.34 mm; SL = 0.15 mm; WL = 0.59 mm; PrW = 0.20 mm; MW = 0.22 mm; PTL = 0.14 mm; PTH = 0.14 mm; PTW = 0.14 mm; CI = 81; SI = 53; PI = 104.

Description

Worker

Lateral margins of cranium subparallel. Occipital carina only distinct ventrally. Clypeal process absent; clypeal margin linear, entire. Mandibles short relative to head (MI = 47–53); three teeth present. Large, tapering basal seta absent from mandible; subapical tapering seta present, no longer than adjacent setae. Maxillary palp 1-merous. Scape short, less than ½ length of cranium (SI = 60–61), somewhat expanded towards apex. Pedicel length distinctly greater than that of basal flagellomere. Flagellum submoniliform; length of antennomere 3 subequal to respective lengths of antennomeres 4–6, with lengths of antennomeres 7–11 greater than those of antennomeres 4–6; antennomere 12 (i.e., apical flagellomere) 2× as long as antennomere 11. In dorsal view, pronotal margins moderately convex, pronotal width only slightly greater than mesonotal width. Pronotal dorsum planar, not elevated above dorsal mesonotal vertex. Lateral

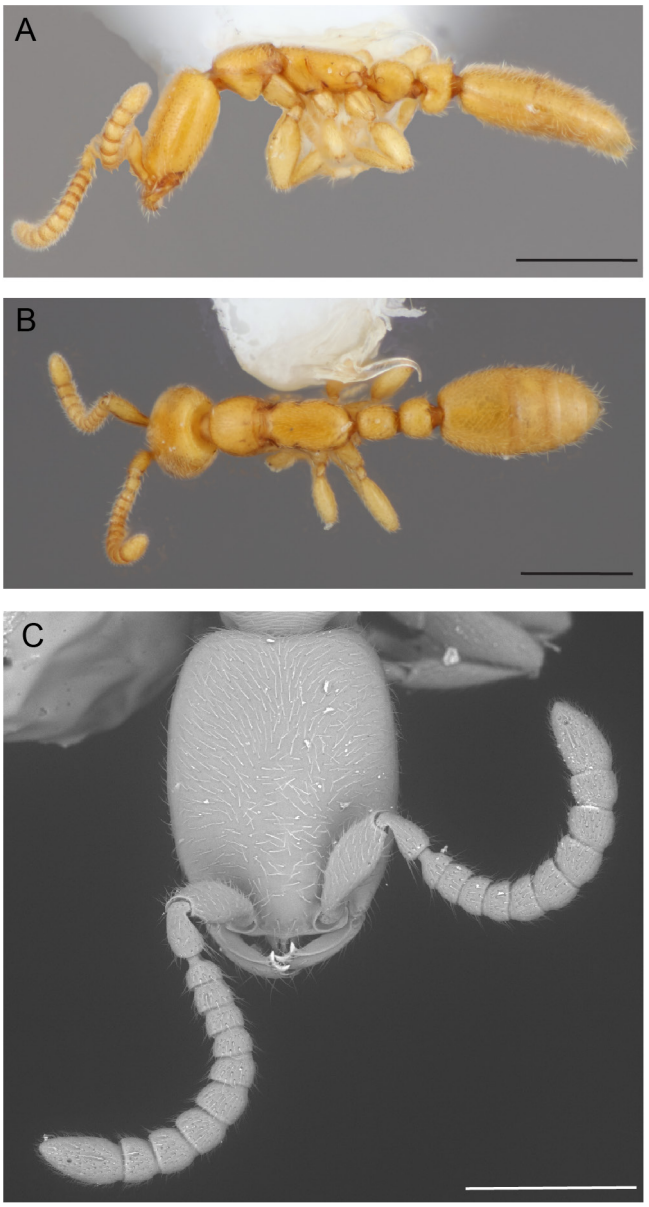

Fig. 19. *Leptanilla phthirigyna* sp. nov., holotype, worker (CSUENT6000054). **A**. Profile view. **B**. Dorsal view. **C**. Full-face view. Scale bars: A–B = 0.4 mm; C = 0.2 mm.

margins of mesonotum and metapectal-propodeal complex subparallel in dorsal view; mesonotum not constricted anteriorly. Meso-metapleural suture absent dorsally; present as signum in profile view. Bulla not extending anterad propodeal spiracle. Propodeum convex in profile view; propodeal declivity indistinct from dorsum; posterolateral corners of propodeum rounded. Tarsomeres longer than broad. Meso- and metatibial spur formula 1b,2b. Anterior margin of abdominal segment II linear in dorsal view. Length of abdominal segment II greater than breadth in dorsal view, distinct dorsal node present; margins parallel in dorsal view; subpetiolar process present, not lamellate, anterior face not concave in profile view. Length of abdominal segment II (PTL = 0.08–0.09 mm) subequal to that of abdominal segment III

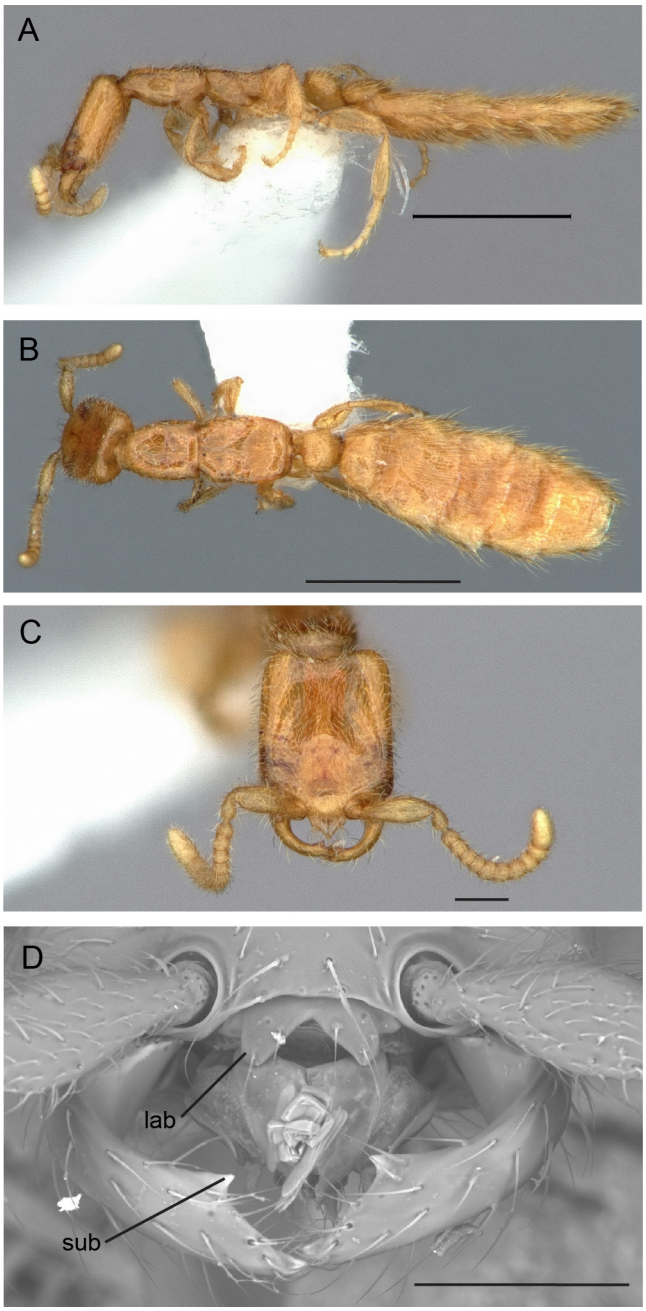

Fig. 20. *Leptanilla phthirigyna* sp. nov., paratype, gyne (CASENT0842890). **A**. Profile view. **B**. Dorsal view. **C**. Full-face view. Abbreviations: lab = labrum; sub = subapical tooth. Scale bars: A–B = 0.5 mm; C–D = 0.1 mm.

(PPL = 0.08 mm); abdominal sternite III not projecting ventrad abdominal sternite II. Length and breadth of abdominal segment III subequal in dorsal view. Breadth of abdominal segment III approximately half that of abdominal segment IV in dorsal view (TI1 = 43–48). Abdominal tergites IV–VII visible in posterodorsal view. Anteroposterior length of abdominal tergite IV twice anteroposterior length of abdominal tergite V in dorsal view. Abdominal tergite IV not constricted anteriorly. Anteroposterior lengths of abdominal tergites V–VI subequal; anteroposterior length of abdominal tergite VII much less than that of abdominal tergite VI. Sculpture largely absent. Vestiture consisting of short subdecumbent setae, longer and more abundant on gaster than on remainder of soma. Coloration yellowish.

Gyne

Labrum deeply emarginate. Cranium in full-face view rectangular; occipital margin emarginate. Clypeal process absent. Mesonotum not laterally delimited from mesopleuron by furrow. In dorsal view, breadth of mesonotum greater than that of pronotum or metanotal-propodeal complex. Propodeum without distinct declivity. Abdominal segment II subsessile, abdominal postsclerites II not constricted anteriorly, dorsal apex of petiolar node exceeding dorsal apex of abdominal tergite III; dorsal node situated towards anterior of abdominal segment II. In dorsal view, abdominal segment III conspicuously narrower than abdominal segment IV, supra-axial relative to posterad abdominal segments; lengths of abdominal postsclerites IV and VII subequal, greater than abdominal postsclerites III and V–VI. Vestiture dense, with setae coarse and suberect to subdecumbent on head and mesosoma; setae long, fine, and subdecumbent on metasoma.

Distribution

Known only from the type locality.

Ecology

Like *Protanilla rong* sp. nov., *L. phthirigyna* sp. nov. was collected just below the surface of a termite mound, a microhabitat not previously reported for the Leptanillinae. The discovery of a physogastric gyne (CASENT0842889) confirms phasic brood production in *L. phthirigyna*, as in all other *Leptanilla* for which biology is known. The existence of two gynes in a single putative colony is exceptional for *Leptanilla* but most be considered only circumstantial without further study: the reproductive phases of these two individuals were not synchronized, contrary to the behavior of gynes in confirmed polygynous ants that practice phasic brood production (e.g., the *Cerapachys sulcinodis* species-complex [Dorylinae]; Mizuno *et al.* 2021).

Remarks

The worker of *Leptanilla phthirigyna* sp. nov. most closely resembles that of *Leptanilla okinawensis* Terayama, 2013, differing in the proportions of the pedicel, and in that the subpetiolar process is situated midway along the anteroposterior length of abdominal segment II, rather than posterad that point. The condition of the lateral meso-metapleural suture in *L. okinawensis* is unknown, and this species has not yet been sequenced.

Leptanilla phthirigyna sp. nov. is found by phylogenomic inference to belong to the *Leptanilla revelierii* species-group, corroborated by the absence of a clypeal process and the proportions of abdominal segments IV–VIII. The species belongs to an east Asian radiation of the *Leptanilla revelierii* species-group that also includes *Leptanilla taiwanensis* Ogata *et al.*, 1995 (Fig. 2).

Discussion

Cranial anatomy of *Leptanilla*

Morphology of the anterior cranial margin occupies a continuum across *Leptanilla* (Griebenow *et al.* 2022: fig. 14). In the *Leptanilla revelierii* species-group, the anterior cranial margin is often entire, with

exceptions having either a median divot (Ogata *et al.* 1995: fig. 14), or small anteromedian projection which is itself entire (Leong *et al.* 2018: fig. 4). Furthermore, the clypeus is never demarcated from the frontal area. In other clades of *Leptanilla* for which the worker caste is known, the anterior cranial margin forms a variously projecting process, with the clypeus appearing distinct from the frons as a bulging region and sometimes delimited posteriorly by a signum (as in *Leptanilla belantanoides* sp. nov.).

Most authors have assumed that this anterior process is clypeal (Wong & Guénard 2016; Leong *et al.* 2018; Saroj *et al.* 2022), but with the absence of an epistomal sulcus this assumption cannot be externally confirmed. Micro-computed tomography here demonstrates that the origins of the *M. clypeopalatalis* (0ci1) and *M. clypeobuccalis* (0bu1) in *L. belantanoides* sp. nov. coincide with the posterior margin of the so-called (Griebenow *et al.* 2022; Griebenow 2024) frontoclypeal process, confirming the identity of that process as wholly clypeal. The origins of 0ci1 and 0bu1 in *L. charonea* are comparably positioned to these in *L. belantanoides* sp. nov., unexpectedly showing that the clypeus extends posteriorly between the antennal toruli in the *Leptanilla revelierii* species-group, despite being externally invisible (contrary to Griebenow 2024: 116).

Systematics and phylogeny

The work presented here integrates phylogenomics with morphology and micro-computed tomography to advance alpha taxonomy of the Leptanillinae in Vietnam, along with southern China a unique center of phylogenetic diversity for this enigmatic ant clade. Our detailed description of a *Protanilla* larva, and a male of the *Protanilla bicolor* species-group, are novel contributions to the knowledge of both clades: the latter shows drastic contrast with previously described male *Protanilla*, plus remarkable modification to the penial sclerites observed nowhere else in the Leptanillinae to date.

We increase the number of described leptanilline species in Vietnam from one to six; four are newly described in this study. Vietnam is now known to host two of the five major clades of *Leptanilla* and two of the four major clades of *Protanilla*. Interestingly, the male specimen of *Protanilla* zhg-vn01 (CASENT0842613), collected in Tam Dao National Park, is not recovered as sister to the sequenced exemplar of *Protanilla rong* sp. nov. by the phylogenomic inference presented here, instead sharing a more recent common ancestor with *Protanilla jongi*, which is clearly distinct from *P. rong*. This reveals that *Protanilla* zhg-vn01 is a second, undescribed species belonging to the *Protanilla rafflesi* species-group in northern Vietnam. We do not describe this species as new, as the worker caste remains unknown, although CASENT0106383 may represent the gyne of this species. At least one other undescribed species belonging to the *Protanilla rafflesi* species-group has been collected in southern Vietnam (Bidoup Nui Ba National Park, Lam Dong Province) (A. Yamada pers. obs.).

ML and Bayesian phylogenomic inference here demonstrate that *Leptanilla havilandi* and *L. thai* are distant relatives: *Leptanilla thai* belongs well within the former genus *Yavnella*, along with *Leptanilla laventa* and *Leptanilla belantanoides* sp. nov.; whereas *L. havilandi* is sister to the former *Noonilla*, known only from males, and shares a more recent common ancestor with the *Leptanilla revelierii* species-group than with the *Leptanilla thai* species-group (Fig. 2). While the slanted anterior surface of the worker subpetiolar process in *L. havilandi* differs from every known worker within the *Leptanilla thai* species-group, the interspecific variation of the subpetiolar process across worker *Leptanilla* means that we cannot assume that the as-yet unknown worker caste in other representatives of the *Leptanilla havilandi* species-group conforms to this condition. These two clades therefore cannot be considered consistently distinguishable in the worker caste and are not together monophyletic to the exclusion of the *Leptanilla revelierii* species-group, in which worker phenotype consistently contrasts with that the *Leptanilla thai* species-group and *Leptanilla havilandi* species-group. These morphological observations, here contextualized by robust model-based phylogeny, affirm the synonymy of *Yavnella* and *Noonilla* with *Leptanilla* (Griebenow 2024: 128) to ensure higher taxa in the Leptanillini that are

reciprocally monophyletic. *Scyphodon* was not included in phylogenomic inference here, and so the synonymy of that genus with *Leptanilla* is unaddressed by these analyses.

The sister-group relationship and short branches revealed between the worker of *Leptanilla belantanoides* sp. nov. (CASENT0842867) and the putative male (CASENT0842868) strongly indicates their conspecificity but does not confirm it with total certainty. This is since multiple related species in the *Leptanilla thai* species-group could exist in sympatry in Cuc Phuong National Park. As precedent, six putative undescribed species of the *Leptanilla thai* species-group occur in Taninthayi National Park (Rakhine, Burma), all known only from males. Nonetheless, the patristic distance between CASENT0842867 and CASENT0842868 expressed in number of expected substitutions per site across all ML analyses ($\bar{x}$ = 0.00172) is less than that observed between the sympatric sister species *Leptanilla charonea* and *Leptanilla* cf. *zaballosi* ($\bar{x}$ = 0.00858) as inferred in these selfsame analyses, of other syntopic sister morphospecies such as *Leptanilla* zhg-bt01 and CASENT0842862 ($\bar{x}$ = 0.00479) or *Leptanilla* cf. zhg-mm10 and *Leptanilla* zhg-mm14 ($\bar{x}$ = 0.00249), or between the three included sympatric specimens of *Protanilla* zhg-my01 ($\bar{x}$ = 0.00618). The greatest patristic distance among the four specimens of *Protanilla lini* included in ML analyses is considerably greater, but as these originated in allopatry (across the Ryukyu and Amami Islands) this distance is inequivalent to that observed between the worker and putative male of *L. belantanoides* sp. nov. We therefore describe CASENT0842868, CASENT0842869, and CASENT0883690 as *L. belantanoides* in the absence of positive evidence that this is not so.

Maximum-likelihood and Bayesian inference reveal that the putative grasping function of the profemur evolved twice in the *Leptanilla thai* species-group (Fig. 2): in *Leptanilla belantanoides* sp. nov., and once in an undescribed clade so far known only from northern Thailand. That the proximal curvature of the male profemur in these lineages of the *Leptanilla thai* species-group serves to secure the male to the gyne during copulation is speculative, since copulation has never been observed in the Leptanillinae. Modification of the male profemur in the *Leptanilla havilandi* species-group (Griebenow 2024: fig. 29a), *Leptanilla najaphalla* species-group (Griebenow 2024: fig. 42b), or *Leptanilla* ci01 (Griebenow 2024: fig. 31) is more extreme, and difficult to account for except as the result of sexual selection.

While beyond the geographical focus of this paper, the revelation of the phylogenetic position of *Protanilla izanagi* merits discussion. Griebenow (2024: 127) left this species incertae sedis within *Protanilla* on account of its bizarre mouthparts, noting the conformity of the post-cephalic soma to norms of the *Protanilla rafflesi* species-group and *Protanilla bicolor* species-group, and speculating that molecular data would reveal *P. izanagi* to be a member of the former clade (Griebenow 2024: 128). The phylogenomic inferences here presented instead demonstrate that *P. izanagi* is outside the *Protanilla rafflesi* species-group and sister to *Protanilla* zhg-th02, an undescribed male singleton from central Thailand. As noted by Griebenow (2024: 121), this morphospecies deviates conspicuously from the male diagnoses for both the *Protanilla rafflesi* species-group and *Protanilla bicolor* species-group while certainly not being an exemplar of the *Protanilla taylori* species-group. *Protanilla* zhg-th02 displays an oblate-trapezoidal clypeus and an elongate, acuminate mandible, both conditions unique among male Leptanillinae, implying that the unknown worker caste of this morphospecies shares these apomorphies with *P. izanagi*. The geographical disjunction of *P. izanagi* and *Protanilla* zhg-th02 is presumably an artifact of acquisition bias, implying that the *Protanilla izanagi* species-group is widespread throughout temperate and tropical eastern Asia, including Vietnam. Given collection records of *P. izanagi*, we recommend *lavage de terre* throughout Vietnam and neighboring countries to acquire kin of this enigmatic ant.

Acknowledgments

We first gratefully acknowledge the collecting efforts of Michael Branstetter and Katsuyuki Eguchi, which resulted in specimens integral to this study; and Brian Fisher (CAS) and Nguyen Van Sinh (IEBR)

along with associated organizers of Ant Course 2022, during which the specimens from Cuc Phuong National Park examined here were collected. We thank Jadranka Rota (MZLU), Debbie Jennings (ANIC), Federica Turco (ANIC), Masashi Yoshimura (OIST), Kevin Williams (CSCA), Bonnie Blaimer (ZMHB), Brian Fisher (CASC), Chris Darling (ROME), Benoit Guénard (HKUBM), Po-Wei Hsu (NCUE), Majid Moradmand (ZMUI), Yu Hisasue, José María Gómez-Durán, and the staff of Flora & Fauna International (Burma) for collecting, loaning or donating specimens; and are also grateful to Bui Tuan Viet, Katsuyuki Eguchi, Michael Ohl, Christian Rabeling, and Michael Sharkey for material sequenced by Borowiec *et al*. (2019), from which molecular data were also incorporated into phylogenetic inference published herein. We additionally thank Michael Branstetter for his assembly of raw UCE reads used for phylogenomic inference; the Okinawa Institute of Science and Technology Graduate University (OIST) Imaging Section for providing access to the Zeiss Xradia μ-CT scanner and REM facilities, along with Shinya Komoto and Toshiaki Mochizuki for general support; and Jason Bond for granting access to the Hitachi TM4000. Finally, we thank Phil Ward and Marek Borowiec for their conceptual advice, and logistical and monetary support, for this project. AD gratefully acknowledges support from the IEBR Fund for the Promotion of Young Researchers (IEBR.NV.02-23); AR is thankful for an international postdoctoral fellowship of the Japan Society for the Promotion of Science (JSPS, 2023–2024), and for a PhD fellowship of the Evangelisches Studienwerk Villigst eV that enabled participation in AntCourse; ZG is grateful for an Ernst Mayr Travel Grant (May 2020) to consult specimens of the Leptanillinae at the Museum of Comparative Zoology, Harvard University, Cambridge, MA. Part of this work was conducted under the framework of the memorandum of understanding (MOU) on academic research cooperation between Tokyo Metropolitan University (TMU) and Institute of Ecology and Biological Resources (IEBR). Funding for the research presented here was supported in part by the NSF grant DEB-1932405 to P.S. Ward, Asahi Glass Foundation fund FY2017-FY2020 to K. Eguchi, UC Davis Department of Entomology, the Helmsley Charitable Trust, and the SI Global Genome Initiative.

References

Aberer A.J., Kobert K. & Stamatakis A. 2014. ExaBayes: Massively parallel Bayesian tree inference for the whole-genome era. *Molecular Biology and Evolution* 31 (10): 2553–2556. https://doi.org/10.1093/molbev/msu236

AntWeb 2024. AntWeb. Version 8.114. California Academy of Science. Available from https://www.antweb.org [accessed 22 Feb. 2025].

Aswaj P., Anoop K. & Priyadarsanan D.R. 2020. First record of the rarely collected ant *Protanilla gengma* Xu, 2012 (Hymenoptera, Formicidae, Leptanillinae) from the Indian subcontinent. *Check List* 16 (6): 1621–1625. https://doi.org/10.15560/16.6.1621

Bankevich A., Nurk S., Antipov D., Gurevich A.A., Dvorkin M., Kulikov A.S., Lesin V.M., Nikolenko S.I., Pham S., Prjibelski A.D., Pyshkin A.V., Sirotkin A.V., Vyahhi N., Tesler G., Alekseyev M.A. & Pevzner P.A. 2012. SPAdes: A new genome assembly algorithm and its applications to single-cell sequencing. *Journal of Computational Biology* 19 (5): 455–477. https://doi.org/10.1089/cmb.2012.0021

Baroni Urbani C. 1977. Materiali per una revisione della sottofamiglia Leptanillinae Emery (Hymenoptera: Formicidae). *Entomologica Basiliensia* 2: 427–488.

Barraclough T.G. 2019. *The Evolutionary Biology of Species*. Oxford University Press, Oxford. https://doi.org/10.1093/oso/9780198749745.001.0001

Beutel R.G., Friedrich F., Yang X.-K. & Ge S.-Q. 2014. *Insect Morphology and Phylogeny: A Textbook for Students of Entomology*. Walter de Gruyter, Berlin. https://doi.org/10.1515/9783110264043

Billen J., Bauweleers E., Hashim R. & Ito F. 2013. Survey of the exocrine system in *Protanilla wallacei* (Hymenoptera, Formicidae). *Arthropod Structure & Development* 42 (3): 173–183. https://doi.org/10.1016/j.asd.2013.01.001

Bolton B. 1990. The higher classification of the ant subfamily Leptanillinae (Hymenoptera: Formicidae). *Systematic Entomology* 15 (3): 267–282. https://doi.org/10.1111/j.1365-3113.1990.tb00063.x

Borowiec M.L. 2016. AMAS: A fast tool for alignment manipulation and computing of summary statistics. *PeerJ* 4: e1660. https://doi.org/10.7717/peerj.1660

Borowiec M.L. 2019. Spruceup: Fast and flexible identification, visualization, and removal of outliers from large multiple sequence alignments. *Journal of Open Source Software* 4 (42): 1635. https://doi.org/10.21105/joss.01635

Borowiec M.L., Rabeling C., Brady S.G., Fisher B.L., Schultz T.R. & Ward P.S. 2019. Compositional heterogeneity and outgroup choice influence the internal phylogeny of the ants. *Molecular Phylogenetics and Evolution* 134: 111–121. https://doi.org/10.1016/j.ympev.2019.01.024

Branstetter M.G., Longino J.T., Ward P.S. & Faircloth B.C. 2017. Enriching the ant tree of life: Enhanced UCE bait set for genome-scale phylogenetics of ants and other Hymenoptera. *Methods in Ecology and Evolution* 8 (6): 768–776. https://doi.org/10.1111/2041-210X.12742

Brues C.T. 1925. *Scyphodon*, an anomalous genus of Hymenoptera of doubtful affinities. *Treubia* 6 (2): 93–96.

Castresana J. 2000. Selection of conserved blocks from multiple alignments for their use in phylogenetic analysis. *Molecular Biology and Evolution* 17 (4): 540–552. https://doi.org/10.1093/oxfordjournals.molbev.a026334

Chernomor O., von Haeseler A. & Minh B.Q. 2016. Terrace aware data structure for phylogenomic inference from supermatrices. *Systematic Biology* 65 (6): 997–1008. https://doi.org/10.1093/sysbio/syw037

Cignoni P., Callieri M., Corsini M., Dellepiane M., Ganovelli F. & Ranzuglia G. 2008. MeshLab: an open-source mesh processing tool. *In*: *Eurographics Italian Chapter Conference*: 129–136. https://doi.org/10.2312/LocalChapterEvents/ItalChap/ItalianChapConf2008/129-136

Cruaud A., Nibelet S., Arnal P., Weber A., Fusu L., Gumovsky A., Huber J., Polaszek A. & Rasplus J.-Y. 2019. Optimized DNA extraction and library preparation for minute arthropods: Application to target enrichment in chalcid wasps used for biocontrol. *Molecular Ecology Resources* 19 (3): 702–710. https://doi.org/10.1111/1755-0998.13006

Duwe V.K., Vu L.V., von Rintelen T., von Raab-Straube E., Schmidt S., Nguyen S.V., Vu T.D., Do T.V., Luu T.H., Truong V.B., Di Vincenzo V., Schmidt O., Glöckler F., Jahn R., Lücking R., von Oheimb K.C.M., von Oheimb P.V., Heinze S., Abarca N., ... & Häuser C.L. 2022. Contributions to the biodiversity of Vietnam – Results of VIETBIO inventory work and field training in Cuc Phuong National Park. *Biodiversity Data Journal* 10: e77025. https://doi.org/10.3897/BDJ.10.e77025

Eguchi K., Viet B.T. & Yamane S. 2014. Generic synopsis of the Formicidae of Vietnam (Insecta: Hymenoptera), Part II – Cerapachyinae, Aenictinae, Dorylinae, Leptanillinae, Amblyoponinae, Ponerinae, Ectatomminae and Proceratiinae. *Zootaxa* 3860 (1): 1–46. https://doi.org/10.11646/zootaxa.3860.1.1

Faircloth B.C. 2016. PHYLUCE is a software package for the analysis of conserved genomic loci. *Bioinformatics* 32 (5): 786–788. https://doi.org/10.1093/bioinformatics/btv646

Glenn T.C., Nilsen R.A., Kieran T.J., Sanders J.G., Bayona-Vásquez N.J., Finger J.W., Pierson T.W., Bentley K.E., Hoffberg S.L., Louha S., Leon F.J.G.-D., Portilla M.A. del R., Reed K.D., Anderson J.L., Meece J.K., Aggrey S.E., Rekaya R., Alabady M., Belanger M. ... & Faircloth B.C. 2019. Adapterama I: Universal stubs and primers for 384 unique dual-indexed or 147,456 combinatorially-indexed Illumina libraries (iTru & iNext). *PeerJ* 7: e7755. https://doi.org/10.7717/peerj.7755

Griebenow Z. 2024. Systematic revision of the ant subfamily Leptanillinae (Hymenoptera, Formicidae). *ZooKeys* 1189: 83–184. https://doi.org/10.3897/zookeys.1189.107506

Griebenow Z.H. 2020. Delimitation of tribes in the subfamily Leptanillinae (Hymenoptera: Formicidae), with a description of the male of *Protanilla lini* Terayama, 2009. *Myrmecological News* 30: 229–250.

Griebenow Z.H. 2021. Synonymisation of the male-based ant genus *Phaulomyrma* (Hymenoptera: Formicidae) with *Leptanilla* based upon Bayesian total-evidence phylogenetic inference. *Invertebrate Systematics* 35 (6): 603–636. https://doi.org/10.1071/IS20059

Griebenow Z.H., Isaia M. & Moradmand M. 2022. A remarkable troglomorphic ant, *Yavnella laventa* sp. nov. (Hymenoptera: Formicidae: Leptanillinae), identified as the first known worker of *Yavnella* Kugler by phylogenomic inference. *Invertebrate Systematics* 36 (12): 1118–1138. https://doi.org/10.1071/IS22035

Griebenow Z.H., Richter A., Kamp T. van de, Economo E.P. & Lieberman Z.E. 2023. Comparative morphology of male genital skeletomusculature in the Leptanillinae (Hymenoptera: Formicidae), with a standardized muscular terminology for the male genitalia of Hymenoptera. *Arthropod Systematics & Phylogeny* 81: 945–1018.

Guénard B., Weiser M.D., Gomez K., Narula N. & Economo E.P. 2017. The Global Ant Biodiversity Informatics (GABI) database: synthesizing data on the geographic distribution of ant species (Hymenoptera: Formicidae). *Myrmecological News* 24: 83–89.

Hoang D.T., Chernomor O., von Haeseler A., Minh B.Q. & Vinh L.S. 2018. UFBoot2: Improving the ultrafast bootstrap approximation. *Molecular Biology and Evolution* 35 (2): 518–522. https://doi.org/10.1093/molbev/msx281

Hsu P.-W., Hsu F.-C., Hsiao Y. & Lin C.-C. 2017. Taxonomic notes on the genus *Protanilla* (Hymenoptera: Formicidae: Leptanillinae) from Taiwan. *Zootaxa* 4268 (1): 117–130. https://doi.org/10.11646/zootaxa.4268.1.7

Ito F., Hashim R., Mizuno R. & Billen J. 2022. Notes on the biology of *Protanilla* sp. (Hymenoptera, Formicidae) collected in Ulu Gombak, Peninsular Malaysia. *Insectes Sociaux* 69 (1): 13–18. https://doi.org/10.1007/s00040-021-00839-z

Kalyaanamoorthy S., Minh B.Q., Wong T.K.F., von Haeseler A. & Jermiin L.S. 2017. ModelFinder: Fast model selection for accurate phylogenetic estimates. *Nature Methods* 14 (6): 587–589. https://doi.org/10.1038/nmeth.4285

Kass J.M., Guénard B., Dudley K.L., Jenkins C.N., Azuma F., Fisher B.L., Parr C.L., Gibb H., Longino J.T., Ward P.S., Chao A., Lubertazzi D., Weiser M., Jetz W., Guralnick R., Blatrix R., Lauriers J.D., Donoso D.A., Georgiadis C. ... & Economo E.P. 2022. The global distribution of known and undiscovered ant biodiversity. *Science Advances* 8 (31): eabp9908. https://doi.org/10.1126/sciadv.abp9908

Katoh K. & Toh H. 2010. Parallelization of the MAFFT multiple sequence alignment program. *Bioinformatics* 26 (15): 1899–1900. https://doi.org/10.1093/bioinformatics/btq224

Kück P., Garcia F.H., Misof B. & Meusemann K. 2011. Improved phylogenetic analyses corroborate a plausible position of *Martialis heureka* in the ant tree of life. *PLoS ONE* 6 (6): e21031. https://doi.org/10.1371/journal.pone.0021031

Kugler J. 1987. The Leptanillinae (Hymenoptera: Formicidae) of Israel and a description of a new species from India. *Israel Journal of Entomology* 20: 45–57.

Kutter H. 1948. Beitrag zur Kenntnis der Leptanillinae (Hym. Formicidae). Eine neue Ameisengattung aus Süd-Indien. *Mitteilungen der Schweizerischen Entomologischen Gesellschaft* 21: 286–295.

Leong C.-M., Yamane S. & Guénard B.S. 2018. Lost in the city: discovery of the rare ant genus *Leptanilla* (Hymenoptera: Formicidae) in Macau with description of *Leptanilla macauensis* sp. nov. *Asian Myrmecology* 10: e010001. https://doi.org/10.20362/AM.010001

López F., Martinez M.D. & Barandica J.M. 1994. Four new species of the genus *Leptanilla* (Hymenoptera: Formicidae) from Spain – relationships to other species and ecological issues. *Sociobiology* 24: 179–212.

Lösel P.D., van de Kamp T., Jayme A., Ershov A., Faragó T., Pichler O., Tan Jerome N., Aadepu N., Bremer S., Chilingaryan S.A., Heethoff M., Kopmann A., Odar J., Schmelzle S., Zuber M., Wittbrodt J., Baumbach T. & Heuveline V. 2020. Introducing Biomedisa as an open-source online platform for biomedical image segmentation. *Nature Communications* 11 (1): 5577. https://doi.org/10.1038/s41467-020-19303-w

Masuko K. 1990. Behavior and ecology of the enigmatic ant *Leptanilla japonica* Baroni Urbani (Hymenoptera: Formicidae: Leptanillinae). *Insectes Sociaux* 37 (1): 31–57. https://doi.org/10.1007/BF02223813

Miller M.A., Pfeiffer W. & Schwartz T. 2010. Creating the CIPRES Science Gateway for inference of large phylogenetic trees. *In*: *2010 Gateway Computing Environments Workshop (GCE)*: 1–8. https://doi.org/10.1109/GCE.2010.5676129

Minh B.Q., Schmidt H.A., Chernomor O., Schrempf D., Woodhams M.D., von Haeseler A. & Lanfear R. 2020. IQ-TREE 2: New models and efficient methods for phylogenetic inference in the genomic era. *Molecular Biology and Evolution* 37 (5): 1530–1534. https://doi.org/10.1093/molbev/msaa015

Mizuno R., Suttiprapan P., Jaitrong W., Yamada A. & Ito F. 2022. Colony composition, phasic reproduction, and queen–worker dimorphism of an oriental non-army ant doryline *Cerapachys sulcinodis* species complex in northern Thailand. *Insectes Sociaux* 69 (1): 19–35. https://doi.org/10.1007/s00040-021-00841-5

Nguyen L.-T., von Haeseler A. & Minh B.Q. 2018. Complex models of sequence evolution require accurate estimators as exemplified with the invariable site plus gamma model. *Systematic Biology* 67 (3): 552–558. https://doi.org/10.1093/sysbio/syx092

Ogata K., Terayama M. & Masuko K. 1995. The ant genus *Leptanilla*: Discovery of the worker-associated male of *L. japonica*, and a description of a new species from Taiwan (Hymenoptera: Formicidae: Leptanillinae). *Systematic Entomology* 20 (1): 27–34. https://doi.org/10.1111/j.1365-3113.1995.tb00081.x

Petersen B. 1968. Some novelties in presumed males of the Leptanillinae (Hym., Formicidae). *Entomologiske Meddelelser* 36: 577–598.

Qian Y.-H., Xu Z.-H., Man P. & Liu G.-L. 2024. Three new species of the ant genus *Leptanilla* (Hymenoptera: Formicidae) from China, with a key to the world species. *Myrmecological News* 34: 21–44.

Rabeling C., Brown J.M. & Verhaagh M. 2008. Newly discovered sister lineage sheds light on early ant evolution. *Proceedings of the National Academy of Sciences* 105 (39): 14913–14917. https://doi.org/10.1073/pnas.0806187105

Rambaut A., Drummond A.J., Xie D., Baele G. & Suchard M.A. 2018. Posterior summarization in bayesian phylogenetics using Tracer 1.7. *Systematic Biology* 67 (5): 901–904. https://doi.org/10.1093/sysbio/syy032

Richter A., Hita Garcia F., Keller R.A., Billen J., Economo E.P. & Beutel R.G. 2020. Comparative analysis of worker head anatomy of *Formica* and *Brachyponera* (Hymenoptera: Formicidae). *Arthropod Systematics & Phylogeny* 78 (1): 133–170. https://doi.org/10.26049/ASP78-1-2020-06

Rohland N. & Reich D. 2012. Cost-effective, high-throughput DNA sequencing libraries for multiplexed target capture. *Genome Research* 22 (5): 939–946. https://doi.org/10.1101/gr.128124.111

Romiguier J., Borowiec M.L., Weyna A., Helleu Q., Loire E., La Mendola C., Rabeling C., Fisher B.L., Ward P.S. & Keller L. 2022. Ant phylogenomics reveals a natural selection hotspot preceding the origin of complex eusociality. *Current Biology* 32 (13): 2942–2947. https://doi.org/10.1016/j.cub.2022.05.001

Saroj S., Arnab Mandi & Dubey A.K. 2022. A new species of the rare ant genus, *Leptanilla* Emery (Hymenoptera: Formicidae) from Eastern Himalaya, India. *Asian Myrmecology* 15: e015005. https://doi.org/10.20362/AM.015005

Satria R., Putri D.H. & Ahda Y. 2023. Genus *Protanilla* Taylor, 1990 (Hymenoptera: Formicidae: Leptanillinae) from Sumatra, with the description of a new species. *Serangga* 28 (1): 69–78.

Snodgrass R.E. 1935. *Principles of Insect Morphology*. Cornell University Press, Ithaca.

Sterling E.J., Hurley M.M. & Minh L.D. 2008. *Vietnam: A Natural History*. Yale University Press, New Haven.

Wong M.K.L. & Guénard B. 2016. *Leptanilla hypodracos* sp. n., a new species of the cryptic ant genus *Leptanilla* (Hymenoptera, Formicidae) from Singapore, with new distribution data and an updated key to Oriental *Leptanilla* species. *ZooKeys* 551: 129–144. https://doi.org/10.3897/zookeys.551.6686

Xu Z.-H. 2012. *Furcotanilla*, a new genus of the ant subfamily Leptanillinae from China with descriptions of two new species of *Protanilla* and *P. rafflesi* Taylor (Hymenoptera: Formicidae). *Sociobiology* 59 (2): 477–491. https://doi.org/10.13102/sociobiology.v59i2.612

Yamada A., Nguyen D.D. & Eguchi K. 2020. Unveiling the morphology of the Oriental rare monotypic ant genus *Opamyrma* Yamane, Bui & Eguchi, 2008 (Hymenoptera: Formicidae: Leptanillinae) and its evolutionary implications, with first descriptions of the male, larva, tentorium, and sting apparatus. *Myrmecological News* 30: 111–124.

Yamada A., Eguchi K. & Van Dang A. 2023. Natural history notes of the rare enigmatic ant *Opamyrma hungvuong*: a first glimpse of their preying behavior on centipedes (Hymenoptera: Formicidae: Leptanillinae). *Asian Myrmecology* 16 (1): 1–14.

Yamane S., Viet B.T., Ogata K., Okido H. & Eguchi K. 2002. Ant fauna of Cuc Phuong National Park, North Vietnam (Hymenoptera: Formicidae). *Bulletin of the Institute of Tropical Agriculture, Kyushu University* 25: 51–62. https://doi.org/10.11189/bita.25.51

Yang Z. 1996. Among-site rate variation and its impact on phylogenetic analyses. *Trends in Ecology & Evolution* 11 (9): 367–372. https://doi.org/10.1016/0169-5347(96)10041-0

Zhong Y. 2024. A new species of the ant genus *Leptanilla* Emery, 1870 (Hymenoptera: Formicidae) from Sichuan Province, China. *Sociobiology* 71 (3): e10478. https://doi.org/10.13102/sociobiology.v71i3.10478

Manuscript received: 8 June 2024
Manuscript accepted: 28 October 2024
Published on: 10 April 2025
Topic editor: Tony Robillard
Section editor: Enrico Schifani
Desk editor: Pepe Fernández

Printed versions of all papers are deposited in the libraries of four of the institutes that are members of the *EJT* consortium: Muséum national d'Histoire naturelle, Paris, France; Meise Botanic Garden, Belgium; Royal Museum for Central Africa, Tervuren, Belgium; Royal Belgian Institute of Natural Sciences, Brussels, Belgium. The other members of the consortium are: Natural History Museum of Denmark, Copenhagen, Denmark; Naturalis Biodiversity Center, Leiden, the Netherlands; Museo Nacional de Ciencias Naturales-CSIC, Madrid, Spain; Leibniz Institute for the Analysis of Biodiversity Change, Bonn – Hamburg, Germany; National Museum of the Czech Republic, Prague, Czech Republic; The Steinhardt Museum of Natural History, Tel Aviv, Israël.

Supplementary files

Supp. file 1. Summary statistics for the 534-locus UCE alignment untrimmed with Spruceup, associated with metadata for each included sequence. https://doi.org/10.5852/ejt.2025.987.2867.13019

Supp. file 2. Parameters for each micro-computed tomographic scan included in this study. https://doi.org/10.5852/ejt.2025.987.2867.13021

.